Multigroup Multicast Precoding for Energy Optimization in SWIPT Systems with Heterogeneous Users

Sumit Gautam, *Student Member, IEEE*, Eva Lagunas, *Senior Member, IEEE*, Ashok Bandi, *Student Member, IEEE*, Symeon Chatzinotas, *Senior Member, IEEE*, Shree Krishna Sharma, *Senior Member, IEEE*, Thang X. Vu, *Member, IEEE*, Steven Kisseleff, *Member, IEEE*, and Björn Ottersten, *Fellow IEEE, IEEE*

The key to developing future generations of wireless communication systems lies in the expansion of extant methodologies, which ensures the coexistence of a variety of devices within a system. In this paper, we assume several multicasting (MC) groups comprising three types of heterogeneous users including Information Decoding (ID), Energy Harvesting (EH) and both ID and EH. We present a novel framework to investigate the multi-group (MG) - MC precoder designs for three different scenarios, namely, Separate Multicast and Energy Precoding Design (SMEP), Joint Multicast and Energy Precoding Design (JMEP), and Per-User Information and/or Energy Precoding Design (PIEP). In the considered system, a multi-antenna source transmits the relevant information and/or energy to the groups of corresponding receivers using more than one MC streams. The data processing users employ the conventional ID receiver architectures, the EH users make use of a non-linear EH module for energy acquisition, while the users capable of performing both ID and EH utilize the separated architecture with disparate ID and non-linear EH units. Our contribution is threefold. Firstly, we propose an optimization framework to i) minimize the total transmit power and ii) to maximize the sum harvested energy, the two key performance metrics of MG-MC systems. The proposed framework allows the analysis of the system under arbitrary given quality of service and harvested energy requirements. Secondly, to deal with the non-convexity of the formulated problems, we transform the original problems respectively into equivalent forms, which can be effectively solved by semi-definite relaxation (SDR) and alternating optimization. The convergence of the proposed algorithms is analytically guaranteed. Thirdly, a comparative study between the proposed schemes is conducted via extensive numerical results, wherein the benefits of adopting SMEP over JMEP and PIEP models are discussed.

Index Terms—Energy optimization, multi-group multicast systems, precoding, simultaneous wireless information and power transmission (SWIPT).

I. INTRODUCTION

A. Motivation

RECENT developments related to wireless communication systems of current and evolving generations have exposed several critical issues such as growing performance and capacity demands, complicated hardware designs, and need for energy-efficient architectures. Rapid battery drainage at power-limited wireless devices also raise concerns, while addressing the above-mentioned assertive demands. Consequently, two promising energy optimization techniques, namely, energy harvesting (as a recharging alternative) and minimization of power consumption (for enhancing the battery lifetime), respectively, may prove useful to address the aforementioned challenges [1], [2]. Incorporation and implementation of such methods is likely to be considered essential from the Internet-of-Things (IoT) perspective [3]–[5]. The observed transitional trend of customers between any consequent generations of wireless mobile communications, i.e., NG to (N+1)G (where N = 1, …, 4), reveals that it is almost impossible to switch directly into an advanced and superior technology altogether [6]. This implies that an intermediate time period is almost

certain, until all the customer devices have been upgraded to the technology with the latest mobile generation. In the context of wireless energy harvesting (EH) devices based on radio-frequency (RF), e.g., sensors, smart devices and home gateways all under the same wireless network, we envision that a similar trend will be observed upon their launch. Therefore, it is necessary to make sure that different kinds of concerned devices such as information decoding (ID) specific, explicit to EH, and the ones performing ID and EH simultaneously, co-exist within the wireless networks and derive maximal gains, which is the main focus of this paper.

B. Related Works

Traditional information processing units have been shown to perform significantly better within a Multiple-Input Single-Output (MISO) set-up [7], in comparison to a one-to-one device communication scheme based on a single antenna. In [8], Varshney presented a framework to spark interest in the possibility of concurrent information and energy transmission using the RF signals. This work was later extended to multi-user MISO case in [1], [9]. There has been a growing research interest in the field of simultaneous wireless information and power transmission (SWIPT) over the past decade [10]. A major outcome in this direction points towards the inability of the traditional ID receivers to harvest RF energy and thus, this calls for a change in the classical receiver architecture. In this context, researchers have proposed several interesting receiver designs for enabling SWIPT [11], with the four most viable designs being time-switching (TS), power-splitting (PS), separated architecture (SA) and integrated architecture

(IA). The complex circuitries associated with TS, PS, and IA-based receivers for SWIPT includes one or more additional optimization parameter(s) in order to segregate the received signal for carrying out either distinct or simultaneous ID and EH operations. In this regard, the SA-based SWIPT receivers may come in handy to reduce the architectural demands within the transmit-receive systems.

In order to combat the aforementioned challenges, transmit precoding is a potential technique not only for enhancing the channel capacity and diversity, but also for mitigating interference in the context of multi-user MISO systems [12]. The authors in [1] presented a framework to jointly optimize the transmit beamforming and the receive power splitting (PS) ratio for SWIPT in MISO systems. Furthermore, energy efficiency optimization was considered in [13] with the same set-up targeting the Zero-Forcing (ZF) beamforming. In [14], Xu *et. al.*, studied the maximization of harvested energy for multi-user MISO SWIPT systems considering SA receiver architecture with a goal to optimize the ID and EH beamforming strategies. However, the above-mentioned works do not consider the non-linear EH model for SWIPT, which is more realistic in comparison to its counterpart linear EH model. In [15], the advantages of employing precoding in MISO broadcast channels were presented for SWIPT systems, whereas joint multi-objective optimization for transmit precoding and receiver TS design was proposed in [16] considering a similar scenario with MISO and SWIPT systems.

Multi-group (MG) Multicasting (MC) is another promising technique to significantly improve the system performance. In [17], the authors proposed a framework for MG-MC beamformer design in the context of multiple-input single-output – orthogonal frequency division multiplexing (MISO-OFDM) with antenna selection. The benefits of precoding in a MG-MC scenario were demonstrated in [18]–[20]. The authors in [21] considered precoding for MG-MC with a common message to study the problem of maximization of weighted sum-rate (WSR) for two schemes where the transmitter superimposes common and multicast messages, and transmitter concatenates the multicast message vector with the common message, respectively. However, it was shown in [12] that an MC precoding problem is NP-hard by nature, even for a single group multicast. Several works have discussed joint information and energy transmission in the MG-MC scenario [22]–[24], however, with an assumption of a linear EH module. In [25], the authors studied SWIPT in MISO MG-MC system where each receiver employs the PS SWIPT receiver architecture for investigating the joint MC beamforming and receive power splitting problem to minimize the total transmit power under SINR and EH constraints. A framework to investigate PS-based SWIPT MC was presented in [26] with individual QoS constraints to meet the demands of energy sustainable IoT devices. It is noteworthy that these works do not consider the coexistence of different user types in the case of MG-MC within the MISO–SWIPT scenario.

C. Contributions

In this paper, we consider a MISO MG-MC precoding based-system wherein a transmit source equipped with mul-tiple antennas provides coverage to multiple users with the help of beamforming through adequate precoder designs. We investigate the problems of minimization of total transmit power and maximization of sum-harvested energy (by the intended users), respectively, in three different scenarios incorporating the coexistence of heterogeneous users comprising three different types. Both problems are found to be non-convex in nature, such that in order to achieve a feasible (optimal or sub-optimal) solution, adequate relaxations and/or transformations are required. In this regard, we obtain reasonable solutions to the formulated problems with the help of semidefinite relaxation (SDR) and a slack variable replacement (SVR) technique. A comparative study between the three proposed scenarios is provided via numerical results based on the obtained solutions, where intensive investigation is carried out using parameter alterations under various practical conditions.

This work builds on the authors' previous publication [27], where the problem of transmit power minimization was addressed considering the three above-mentioned scenarios. As an extension, an alternate form of problem considering the maximization of sum-harvested energy is proposed here to address the concerns related to practical limitations of the prior problem (more details are provided in Section IV). Specifically, the main contributions and novelty of this work are listed below

1) We consider a novel MG-MC precoding framework which deals with the co-existence of three types of users capable of information decoding, energy harvesting, and joint information and energy extraction, respectively. In this context, it is important to mention that most of the existing works in the literature do not consider co-existence of multiple user types for analysis.

2) In order to introduce tractability in the minimization of the total transmit power, we provide adequate transformation to simplify the non-linear EH constraint to a linear form. Without loss of generality, this transformation may come in handy to solve similar problems with non-linear EH constraints. With the help of SDR, the problem is further alleviated to an easily solvable convex-form. In comparison to other works, this paper provides more practically oriented problem formulation for the minimization of total transmit power with the consideration of non-linear EH constraint.

3) Taking into consideration the practical implementation concerns of preceding problem, we formulate a sum-harvested energy maximization problem with a non-linear objective and transmit power limitation, in addition to other necessary constraints introduced earlier. In this context, we propose a slack variable replacement (SVR) technique (in conjunction with well-known SDR method) to make the problem tractable, which is then solved efficiently using an iterative algorithm. On the other hand, a simpler problem with linear EH objective and constraint is considered in most of the existing works that analyze the MG-MC framework.

4) Considering the existing works in the literature, it is noteworthy that an investigative comparison between
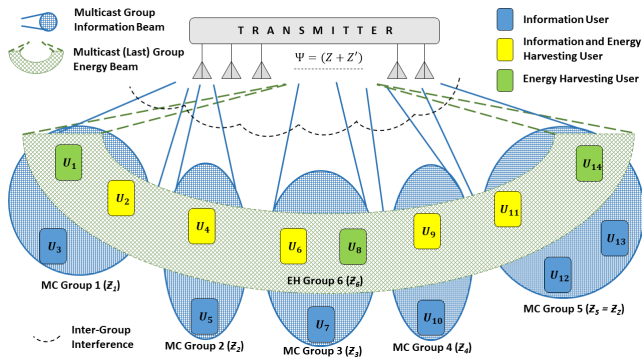
Fig. 1. System model for Separate Multicast and Energy Precoding Design (SMEP). Herein, the intended EH users are served using the corresponding MC beam (blue) as well as a dedicated power beam (green).
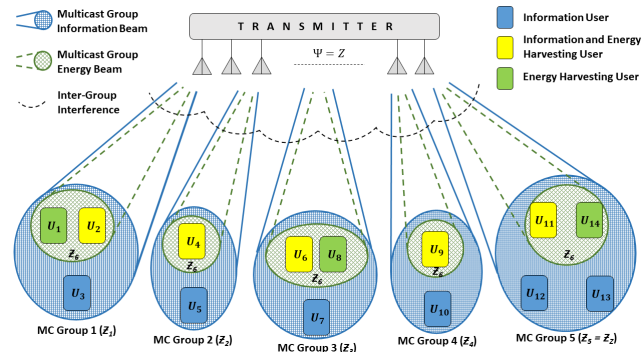

Fig. 2. In Joint Multicast and Energy Precoding Design (JMEP), the EH users are categorized within the stipulated MC groups and all the users are served by their corresponding MC beam (blue). Note that there is/are no separate power beam(s) (green) as such, however, we have depicted the same for convenience to distinguish between the three types of wireless users.
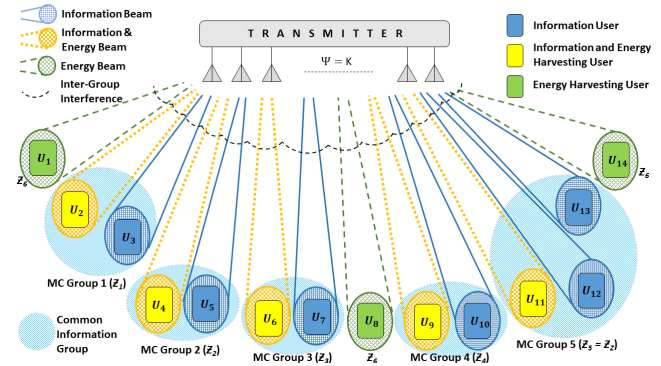

Fig. 3. The system model for Per-User Information and/or Energy Precoding Design (PIEP) consists of dedicated precoders for each user. It is noteworthy that multiple transmissions of common message may occur while serving the set of users within the corresponding MC group.

II. SYSTEM MODEL

We consider a multi-group multicasting (MG-MC) system where a transmit source equipped with M antennas serves K single-antenna users $(U_1, \ldots, U_K)$. Each user may be classified within one of the several possible groups, and is expected to perform either of the following operations, namely, information decoding (ID), energy harvesting (EH), or both ID and EH. In case a user performs both ID and EH, it is assumed to be equipped with disparate RF chains responsible for carrying out the desired operations. Such kind of receiver design is often referred to as the separated architecture (SA) in the literature for enabling joint information processing and energy harvesting [11]. In this work, we specifically categorize the ID users among Z multicasting (MC) groups while we assume that all the EH users are classified under the $(Z+1)^{\text{th}}$ group. Note that the users in $(Z + 1)^{\text{th}}$ group may or may not be a part of any other pre-categorized Z MC groups of ID users. In the considered system, a user requesting joint ID and EH operations would participate in any one of the Z MC groups and also in $(Z + 1)^{\text{th}}$ group. With regard to the categorization of users within the groups, several methods may be implemented. In this regard, channel co-linearity and orthogonality based user grouping is considered in [29] where initially $(Z + 1)$ users (same as number of groups) with most orthogonal channels are considered as different groups. Further, the unallocated users are assigned to the groups based on co-linearity with the existing users in the groups. In [30], the authors consider message based user grouping where it is proved that ad-hoc user grouping is optimal for massive MIMO systems under max-min SINR design criterion. Regarding the categorization of users within specific groups in this work, naturally the users requesting the same (common) information will be a part of same group and thus, distinct groups may be formed and such groups may be assumed to be already known as considered herein. Therefore, for analytical convenience, we assume that all the users are already categorized among various groups and such arrangements are known [22], [23].

We propose and analyze three different precoding design methods for energy optimization, which are discussed below

1) *Separate Multicast and Energy Precoding Design (SMEP)*: In this case, we assume Z multicast infor-

the three proposed scenarios with heterogeneous users (including EH users with non-linear EH modules) has not been presented so far (to the best of authors' knowledge). Herein, we provide a comparative study among the three proposed schemes with separate information and/or energy precoder design, joint information and/or energy precoder design, and per-user information and/or energy precoder design. The latter scheme is considered as the benchmark for comparison purposes. We first draw the comparison between the systems based on a more generalized yet practically-inspired channel modeling scheme, in order to observe their corresponding behaviors under several test cases. Furthermore, we assume uniform linear arrays (ULAs) [28] at the transmitter to test the efficacy of the proposed algorithms over a channel that is simple and can be easily interpreted.

The rest of the paper is organized as follows. Section II provides an insight into the system model. The total transmit power minimization problem and its corresponding solution are presented in Section III, while the sum-harvested energy maximization problem and its (proposed) solution with an iterative algorithm are conferred in Section IV. Numerical results are shown in Section V, followed by concluding remarks in Section VI.

mation groups and an additional group devoted to EH specific users. Thus, we target design of at least $(Z + Z')$ precoders, where we intend to have $Z' = 1$. However, the value of Z' may vary according to the technique used for designing criteria, which will be justified in the later sections.

2) *Joint Multicast and Energy Precoding Design (JMEP)*: Herein, no exclusive precoder is present for EH specific users. In particular, we target the design of Z multicast precoders taking into account the information and/or energy demands of the corresponding users[1].

3) *Per-User Information and/or Energy Precoding Design (PIEP)*: We assume in this case that each user is served by single dedicated precoder. Therefore, we target the design of K precoders (equal to the number of users). This case is very unlikely in practice but is considered as a baseline for comparison purposes.

For illustration purpose, we consider an example with $K = 14$ users, where 6 users are ID specific, 3 users only harvest energy, and 5 users have joint ID and EH capabilities, M transmit antennas (with $M \geq K$ for PIEP to be feasible), and $Z = 5$ MC groups. Correspondingly, the system set-up for the aforementioned three scenarios (SMEP, JMEP, and PIEP) are depicted in Fig. 1, Fig. 2, and Fig. 3, respectively. Let $\mathcal{Z}_k$ denote the kth multicast users' group. Let us also define the following variable to assist the precoding design metrics (i.e., number of precoders) in three cases interchangeably

$$\Psi = \begin{cases} Z + Z' & : \quad \text{SMEP.} \\ Z & : \quad \text{JMEP.} \\ K & : \quad \text{PIEP.} \end{cases} \quad (1)$$

Each ID or joint ID and EH user belongs to only the MC group, i.e., $\mathcal{Z}_k \cap \mathcal{Z}_\ell = \varnothing$, $\forall k, \ell = \{1, \ldots, \Psi\}$ and $k \neq \ell$; whereas in case of EH, the user harvests energy using all the possible multicast signals[2].

The antenna array at the transmitter emits the signal $\mathbf{x}(t) = \sum_{k=1}^{\Psi} \mathbf{w}_k a_k(t)$, where $\mathbf{w}_k$ is the related $M \times 1$ complex precoding weight vector for the users in group $\mathcal{Z}_k$, and $a_k(t)$ is the corresponding information and/or energy signal. Additionally, we assume that the information and/or energy signals for each group $\{a_k(t)\}_{k=1}^{\Psi}$ are mutually uncorrelated to each other with zero mean and unit variance, $\sigma_{a_k}^2 = 1$. The corresponding ID and/or EH signals may be separately designed according to the framework proposed in [31]. Distinct ID and EH signal forms motivate the use of SA-based devices. The total transmitted power can thus be given by $\sum_{k=1}^{\Psi} \mathbf{w}_k^H \mathbf{w}_k$.

The received signal at the ith user is given by $y_i(t) = \mathbf{g}_i^H \mathbf{x}(t) + n_{R,i}(t)$, where $\mathbf{g}_i$ is the $M \times 1$ conjugated channel vector for the corresponding receiver and $n_{R,i}(t)$ is the additive white Gaussian noise at the corresponding i^{th} user's receiving antenna equipment with zero mean and variance

---

[1]In JMEP, it is clear that for the EH users without ID request, classifications are performed within the Z MC groups. Regarding categorization of the EH users within the Z groups, certain methods e.g., distance from the nearest transmit antenna, distance from the nearest beam, etc., may be applied. This, however, involves rigorous analysis and is out of the scope of this work.

[2]The other MCs are primarily taken into consideration due to interference causing side-lobes other than the desired MC, which is beneficial for EH.
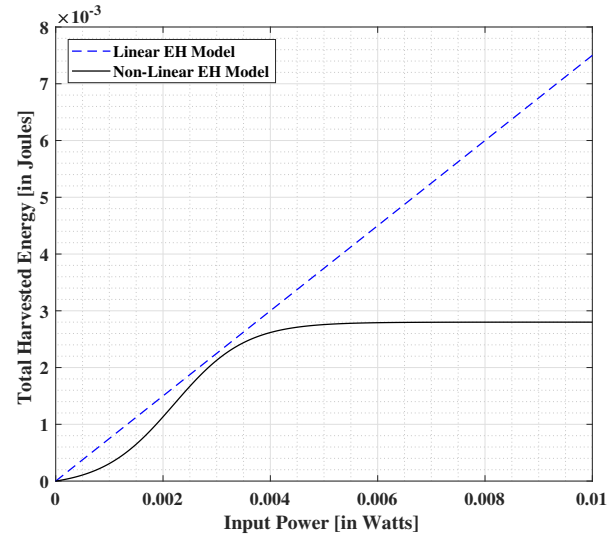

Fig. 4. Comparison between the energy extraction capabilities of linear and non-linear energy harvesting models.

$\sigma_{R,i}^2$. The source signals are assumed to be uncorrelated with $n_{R,i}(t)$. The signal received at the information decoding unit of the ith receiver equipment is expressed as

$$y_{D,i}(t) = \left(\mathbf{g}_i^H \mathbf{x}(t) + n_{R,i}(t)\right) + n_{D,i}(t), \quad (2)$$

where $n_{D,i}(t)$ is the additional zero-mean Gaussian noise with a variance of $\sigma_{D,i}^2$ incurred due to the circuitry and other relevant operations at the ID block of the ith receiver. For i^{th} receiver belonging to the kth multicast group $\mathcal{Z}_k$, the signal-to-interference-and-noise ratio (SINR) is given by

$$\Upsilon_i = \frac{|\mathbf{w}_k^H \mathbf{g}_i|^2}{\sum_{\substack{\ell=1 \\ \ell \neq k}}^{\Psi} |\mathbf{w}_\ell^H \mathbf{g}_i|^2 + \sigma_{R,i}^2 + \sigma_{D,i}^2}. \quad (3)$$

The signal dedicated for EH block of the ith receiver is

$$y_{E,i}(t) = \mathbf{g}_i^H \mathbf{x}(t) + n_{R,i}(t). \quad (4)$$

Therefore, the energy extracted by the EH unit of ith receiver is given as, $\mathcal{E}_i^{\mathcal{L}} = \zeta_i \left(\sum_{k=1}^{\Psi} |\mathbf{w}_k^H \mathbf{g}_i|^2 + \sigma_{R,j}^2\right)$, where $0 < \zeta_i \leq 1$ is the energy conversion efficiency of the EH unit at the corresponding receiver [32]. Note that $\mathcal{E}_i^{\mathcal{L}}$ is theoretically valid in order to represent a linear EH operation, however its practical implementation is questionable. Thus, this calls for the adoption of a non-linear EH model. In this regard, we define the energy harvested at the receiver as follows [33]

$$\mathcal{E}_i^{\mathcal{N}} = \frac{\mathcal{E}'}{1 - \phi} \cdot \left(\frac{1}{1 + e^{(-\alpha(\sum_{k=1}^{\Psi} |\mathbf{w}_k^H \mathbf{g}_i|^2) + \alpha\beta)}} - \phi\right), \quad (5)$$

where $\phi \triangleq \frac{1}{1 + \exp(\alpha\beta)}$, the constant $\mathcal{E}'$ is obtained by determining the maximum harvested energy on the saturation of the EH circuit, and α and β are specific for the capacitor and diode turn-on voltage metrics at the EH circuit. Practically, a standard curve-fitting tool based on analytical data may be used to decide the appropriate values of $\mathcal{E}'$, α, and β. A comparison between the linear and non-linear EH models is depicted in Fig. 4, where $\zeta_i = 0.75$ (for linear EH module),

$\mathcal{E}' = 2.8$ mJ, $\alpha = 1500$, and $\beta = 0.0022$ (for the non-linear EH module) [33], [34]. The non-linearity introduced due to the diode and capacitor elements is observed at lower input power at the EH module while a constant EH operation is seen for higher values of input power which implies the saturation at diode element of the EH module. On the other hand, the linear EH model increases constantly based on the increasing input power at the EH module[3], without considering the saturation points of the circuit elements (such as diode) [33]. We assume normalized time slots to use the terms *power* and *energy* interchangeably.

In the following sections, we formulate the optimization problems corresponding to various precoder designs for minimization of the total transmit power and maximization of sum-harvested energy at the intended users, respectively, for the three scenarios, viz-a-viz., SMEP, JMEP and PIEP. Feasible solutions are obtained by employing suitable transformations and simplifications.

III. TRANSMIT POWER MINIMIZATION

In this section, we minimize the overall transmitted power subjected to minimum SINR and EH constraints at the corresponding users/groups.

A. Problem Formulation

The overall optimization problem for precoder design (encapsulating three aforementioned scenarios) to minimize the total transmit power can be written in its analytical form as

$$(P1): \min_{\{\mathbf{w}_k\}_{k=1}^{\Psi}} \quad \sum_{k=1}^{\Psi} \mathbf{w}_k^H \mathbf{w}_k \qquad (6)$$

$$\text{s.t.} \quad (C1): \frac{\mathbf{w}_k^H \mathbf{G}_i \mathbf{w}_k}{\sum_{\ell \neq k} \mathbf{w}_\ell^H \mathbf{G}_i \mathbf{w}_\ell + \sigma_{R,i}^2 + \sigma_{D,i}^2} \geq \gamma_i,$$

$$\begin{cases} \text{SMEP}: \ \forall i \in \mathcal{Z}_k, \ \forall k \in \{1,\ldots,Z\}, \\ \qquad \forall \ell \in \{1,\ldots,Z+1\}, \\ \text{JMEP}: \ \forall i \in \mathcal{Z}_k, \ \forall k \in \{1,\ldots,Z\}, \\ \qquad \forall \ell \in \{1,\ldots,Z\}, \\ \text{PIEP}: \ \forall i, \forall k, \forall \ell \in \{1,\ldots,K\}, i = k, \end{cases} \quad (7)$$

$$(C2): \mathcal{E}_j^{\mathcal{N}} \geq \xi_j, \forall j \in \mathcal{Z}_{Z+1}, \qquad (8)$$

where γ_i is the SINR threshold at the ith user, ξ_j is the harvested energy demand at j^{th} user (where i can be equal to j for some cases, in general), and $\mathbf{G}_i = \mathbf{g}_i \mathbf{g}_i^H$. It is clear that the formulated problem $(P1)$ is not convex due to constraints $(C1)$ and $(C2)$. Moreover, the feasibility of $(P1)$ is dependent on γ_i and ξ_i, corresponding to $(C1)$ and $(C2)$, respectively, which is additionally constrained by the rank of $\mathbf{G}_i$ [35]. On the other hand, it is interesting to note the hidden linearity aspect within the non-linear EH expression in (5), which can be useful in converting a non-linear EH constraint to a linear form, without loss of generality. The corresponding transformation is provided in (34) of Appendix A. To proceed, we define $\mathbf{w} = [\mathbf{w}_1^T \ \mathbf{w}_2^T \ \ldots \mathbf{w}_\Psi^T]^T$ and $\mathbf{W}_k = \mathbf{w}_k \mathbf{w}_k^H$. With the

[3]This is due to the assumption of a constant energy conversion efficiency at the EH module.

help of these notations, $(P1)$ can be reformulated into a semi-definite programming (SDP) problem as follows

$$(P2): \min_{\{\mathbf{W}_k\}_{k=1}^{\Psi}} \quad \sum_{k=1}^{\Psi} \text{Tr}\{\mathbf{W}_k\} \qquad (9)$$

$$\text{s.t.} \quad (C1): \text{Tr}\{\mathbf{G}_i \mathbf{W}_k\} - \gamma_i \sum_{\ell \neq k} \text{Tr}\{\mathbf{G}_i \mathbf{W}_\ell\}$$

$$\geq \gamma_i (\sigma_{R,i}^2 + \sigma_{D,i}^2),$$

$$\begin{cases} \text{SMEP}: \ \forall i \in \mathcal{Z}_k, \ \forall k \in \{1,\ldots,Z\}, \\ \qquad \forall \ell \in \{1,\ldots,Z+1\}, \\ \text{JMEP}: \ \forall i \in \mathcal{Z}_k, \ \forall k \in \{1,\ldots,Z\}, \\ \qquad \forall \ell \in \{1,\ldots,Z\}, \\ \text{PIEP}: \ \forall i, \forall k, \forall \ell \in \{1,\ldots,K\}, i = k, \end{cases} \quad (10)$$

$$(C2): \sum_{k=1}^{\Psi} \text{Tr}\{\mathbf{G}_j \mathbf{W}_k\} \geq \frac{\xi_j'}{\zeta_j} - \sigma_{R,j}^2,$$

$$\forall j \in \mathcal{Z}_{Z+1}, \qquad (11)$$

$$(C3): \mathbf{W}_k \succeq 0. \qquad (12)$$

The SDP transforms the non-convex $(P1)$ into a convex problem as in $(P2)$, which can be solved using the well-known methods of convex optimization, cf. [36]. For our numerical evaluations, we employ the convex programming tool CVX, wherein we make use of the semi-definite relaxation (SDR) method to simplify $(P2)$ further [37], [38]. It is worth mentioning that in the context of SDR, the well-known procedure is to drop the non-convex constraint of rank$(\mathbf{W}_k) = 1$. Let $\mathbf{W}^\star$ denote the solution of the relaxed problem in $(P2)$. Then, $\mathbf{W}^\star$ is considered the optimal solution iff rank$(\mathbf{W}_k^\star) = 1$ [39]. In this regard, technique like the eigen value decomposition (EVD) [40] or Gaussian randomization [12] may be employed to obtain a unit rank approximation of the precoder metrics.

B. Analysis of Computation Complexity and Motivation for an Alternative Problem Formulation

Assume that the CVX solver encounters the computation complexities of $\nu(\Psi, M, \gamma_i, \xi_i)$ orders for yielding a solution corresponding to $(P2)$. Therefore, the computational complexities for SMEP, JMEP, and PIEP are respectively given by $\mathcal{O}\big((N^3 \cdot (N-1)^2 \cdot K^4)^{\nu(Z+1,M,\gamma_i,\xi_i)}\big)$, $\mathcal{O}\big(((N-1)^5 \cdot K^4)^{\nu(Z,M,\gamma_i,\xi_i)}\big)$, and $\mathcal{O}\big((K^6 \cdot (N-1)^3)^{\nu(K,M,\gamma_i,\xi_i)}\big)$. More discussion is provided in the numerical results section.

The results propound a strong motivation for the practical implementation of proposed framework. However, the possibility of a real-life application (from an indoor-environment perspective) is still doubtful. This is due to the presence of a very hard constraint on harvested energy, i.e., (11) and no limitation on the transmit power. Intuitively, the transmit power has to increase for higher demands of harvested energies. As a result, the total transmit power may not always be guaranteed to respect the Federal Communications Commission (FCC) regulations [41] in general. Therefore, this calls for an alternative formulation focusing on the maximization of the harvested energies of the intended users with a limitation on maximum transmit power, in addition to other necessary constraints. Such kind of problem is more suitable from application view-point

as it is both safe and efficient for the users. In this vein, the relevant developments are outlined in the subsequent section.

IV. Harvested Energy Maximization

We maximize the sum harvested energy by the intended users subjected to predefined SINR and EH constraints at the corresponding users/groups, and an upper limit on the total transmit power.

A. Problem Formulation and Solution

The overall optimization problem (encapsulating the three considered scenarios) to ensure the co-existence of the three user types in MG-MC precoding scheme can subsequently be written in its analytical form as follows

$$(P3): \max_{\{\mathbf{w}_k\}_{k=1}^{\Psi}} \sum_{\forall j \in \mathcal{Z}_{Z+1}} \mathcal{E}_j^{\mathcal{N}} \tag{13}$$

$$\text{s.t. } (C1): \frac{|\mathbf{w}_k^H \mathbf{g}_i|^2}{\sum_{\ell \neq k} |\mathbf{w}_\ell^H \mathbf{g}_i|^2 + \sigma_{R,i}^2 + \sigma_{D,i}^2} \geq \gamma_i,$$

$$\begin{cases} \text{SMEP}: \ \forall i \in \mathcal{Z}_k, \ \forall k \in \{1,\dots,Z\}, \\ \qquad\qquad \forall \ell \in \{1,\dots,Z+1\}, \\ \text{JMEP}: \ \forall i \in \mathcal{Z}_k, \ \forall k \in \{1,\dots,Z\}, \\ \qquad\qquad \forall \ell \in \{1,\dots,Z\}, \\ \text{PIEP}: \quad \forall i, \forall k, \forall \ell \in \{1,\dots,K\}, i=k, \end{cases} \tag{14}$$

$$(C2): \mathcal{E}_j^{\mathcal{N}} \geq \xi_j, \quad \forall j \in \mathcal{Z}_{Z+1}, \tag{15}$$

$$(C3): \sum_{k=1}^{\Psi} \mathbf{w}_k^H \mathbf{w}_k \leq P_{\text{Max}}, \tag{16}$$

where γ_i is the SINR threshold at the ith user, ξ_j is the harvested energy demand at j^{th} user (where i can be equal to j for some cases[4], in general), P_{Max} is the overall available transmit power. Since the problem in $(P3)$ involves a non-linear fractional program, it is non-convex and difficult to solve directly using conventional solvers. In addition, the feasibility of $(P3)$ is dependent on γ_i and ξ_i, which is constrained by the rank of $\mathbf{G}_i$ as well [35]. Moreover, unlike the previous problem in $(P2)$, it is difficult to transform the objective directly into a simpler form, even with the help of SDR. Herein, we intend to find a possibility for an equivalent CVX-solvable problem. In this regard, we propose to transform the fractional form objective function into a slack-variable replacement (SVR) form using the following proposition.

Proposition 1: The maximum achievable sum-harvested energy, $\sum_{\forall j \in \mathcal{Z}_{Z+1}} t_j^\star$, by the intended users can be obtained provided that

$$\max_{\widehat{\mathbf{w}}} \sum_{\forall j \in \mathcal{Z}_{Z+1}} t_j$$

$$= \sum_{\forall j \in \mathcal{Z}_{Z+1}} t_j^\star = \sum_{\forall j \in \mathcal{Z}_{Z+1}} \mathcal{E}_j^{\mathcal{N}}(\widehat{\mathbf{w}}^\star) \tag{17}$$

for $t_j \geq \xi_j$ and $\mathcal{E}_j^{\mathcal{N}}(\widehat{\mathbf{w}}) \geq \xi_j$, where

$$\mathcal{E}_j^{\mathcal{N}}(\widehat{\mathbf{w}}) = \frac{\mathcal{E}'}{1-\phi} \cdot \left(\frac{1}{1 + e^{(-\alpha(\sum_{k=1}^{\Psi} |\mathbf{w}_k^H \mathbf{g}_j|^2) + \alpha\beta)}} - \phi \right), \tag{18}$$

[4]For users within an MC as well as the last group, i can be equal to j.

with $t_j^\star$, $\forall j \in \mathcal{Z}_{Z+1}$, denoting the optimal SVR-parameters, and $\widehat{\mathbf{w}}^\star = \{\mathbf{w}_k^\star\}_{k=1}^{\Psi}$ representing the set of precoders for the respective scenarios, obtained upon the convergence i.e., when the objective function achieves its maximum.

Proof: We first analyze the nature of the objective in $(P3)$, where we observe that the function is concave within the feasible regime. The corresponding proof is provided in Appendix B. Next, we assume that $(P3)$, i.e., [(13)-(16)], is a feasible problem and based on the prior findings, it is obvious that $(P3)$ involves maximization of a concave function subjected to non-linear constraints in (15) and (16). However, the corresponding constraint may be reduced to a simplified (convex) form with the use of adequate transformation or reduction, e.g., SDR. Thus $(P3)$ can subsequently be pared down into a standard convex form (after plausible transformations). Since the objective is a monotonically increasing function of the optimization variables, an optimal (local or global) solution is guaranteed within the feasible set of constraints. Therefore, assuming $\widehat{\mathbf{w}}^\star$ as the optimal set of precoders satisfying the requirements in $(P3)$, the maximum achievable (optimal) objective is given by $\sum_{\forall j \in \mathcal{Z}_{Z+1}} \mathcal{E}_j^{\mathcal{N}}(\widehat{\mathbf{w}}^\star)$. ∎

Proposition 1 provides an adequate and compulsory condition for developing the optimal resource allocation scheme. In particular, based on the original optimization problem with a fractional form-objective function, an equivalent optimization problem with an objective function based on SVR (e.g., $\sum_{\forall j \in \mathcal{Z}_{Z+1}} t_j$, s.t. $\mathcal{E}_j^{\mathcal{N}} \geq t_j$) can be found such that the same solution is achieved for both optimization problems. Moreover, it is explicit that the optimal solution is achieved with equality in (17), and thus we could use this equality condition to validate the optimality of the solution. Hence, rather than tackling the original fractional form-objective function, we develop an alternating algorithm for the equivalent SVR - objective function whilst meeting the conditions in *Proposition 1*. In this regard, we reformulate $(P3)$ with the help of SDR and *Proposition 1*, represented in its mathematical form as

$$(P4): \max_{\substack{\{\mathbf{W}_k\}_{k=1}^{\Psi} \\ \{t_j\}_{\forall j \in \mathcal{Z}_{Z+1}}}} \sum_{\forall j \in \mathcal{Z}_{Z+1}} t_j \tag{19}$$

$$\text{s.t. } (C1): \text{Tr}\{\mathbf{G}_i \mathbf{W}_k\} - \gamma_i \sum_{\ell \neq k} \text{Tr}\{\mathbf{G}_i \mathbf{W}_\ell\}$$

$$\geq \gamma_i(\sigma_{R,i}^2 + \sigma_{D,i}^2),$$

$$\begin{cases} \text{SMEP}: \ \forall i \in \mathcal{Z}_k, \ \forall k \in \{1,\dots,Z\}, \\ \qquad\qquad \forall \ell \in \{1,\dots,Z+1\}, \\ \text{JMEP}: \ \forall i \in \mathcal{Z}_k, \ \forall k \in \{1,\dots,Z\}, \\ \qquad\qquad \forall \ell \in \{1,\dots,Z\}, \\ \text{PIEP}: \quad \forall i, \forall k, \forall \ell \in \{1,\dots,K\}, i=k, \end{cases} \tag{20}$$

$$(C2): \frac{1}{1 + e^{(-\alpha(\sum_{k=1}^{\Psi} \text{Tr}\{\mathbf{G}_j \mathbf{W}_k\}) + \alpha\beta)}}$$

$$\geq t_j\left(\frac{1-\phi}{\mathcal{E}'}\right) + \phi, \quad \forall j \in \mathcal{Z}_{Z+1}, \tag{21}$$

$$(C3): t_j \geq \xi_j, \quad \forall j \in \mathcal{Z}_{Z+1}, \tag{22}$$

$$(C4): \sum_{k=1}^{\Psi} \text{Tr}\{\mathbf{W}_k\} \leq P_{\text{Max}}, \tag{23}$$

$$(C5): \mathbf{W}_k \succeq 0, \tag{24}$$

Algorithm 1 Iterative Algorithm for Harvested Energy Maximization

1: **Initialize**: $\{t_j\}_{\forall j \in \mathcal{Z}_{Z+1}}$, and ϵ as the threshold limit;
2: **REPEAT**
3:    Given $\{t_j\}$, $\forall j$, solve (19)-(24) to obtain $\{\mathbf{W}_k(n)\}_{k=1}^{\Psi}$;
4:    **IF** $(t_j(n) - t_j(n-1) \leq \epsilon)$ & $(n > 2)$
5:      Convergence_1 = **TRUE**;
6:      **RETURN** $\{\mathbf{W}_k^\star\}_{k=1}^{\Psi} = \{\mathbf{W}_k(n-1)\}_{k=1}^{\Psi}$, $t_j^\star = t_j(n-1)$;
7:    **ELSE**
8:      Convergence_1 = **FALSE**;
9:    **END IF**
10:   Given $\{\mathbf{W}_k(n)\}_{k=1}^{\Psi}$, solve (19)-(24) to get $\{t_j(n)\}_{\forall j \in \mathcal{Z}_{Z+1}}$;
11:   **IF** $(t_j(n) - t_j(n-1) \leq \epsilon)$ & $(n > 2)$
12:     Convergence_2 = **TRUE**;
13:     **RETURN** $t_j^\star = t_j(n-1)$, $\{\mathbf{W}_k^\star\}_{k=1}^{\Psi} = \{\mathbf{W}_k(n-1)\}_{k=1}^{\Psi}$;
14:   **ELSE**
15:     $t_j(n+1) = t_j(n)$, $\forall j$, and $n = n + 1$;
16:     Convergence_2 = **FALSE**;
17:   **END IF**
18: **UNTIL** Convergence_1 = **TRUE** & Convergence_2 = **TRUE**.

Algorithm 2 Directional Power Maximization Algorithm (DPMA)

1: **Initialize**: $\{t_j\}_{\forall j \in \mathcal{Z}_{Z+1}}$, $\{\widetilde{\mathbf{w}}_k\}_{k=1}^{\Psi}$, and ϵ;
2: **REPEAT**
3:    Given $\{t_j\}$, $\forall j$, solve (25)-(30) to obtain $\{\mathrm{p}_k(n)\}_{k=1}^{\Psi}$;
4:    **IF** $(t_j(n) - t_j(n-1) \leq \epsilon)$ & $(n > 2)$
5:      Convergence_1 = **TRUE**;
6:      **RETURN** $\{\mathrm{p}_k^\star\}_{k=1}^{\Psi} = \{\mathrm{p}_k(n-1)\}_{k=1}^{\Psi}$, $t_j^\star = t_j(n-1)$;
7:    **ELSE**
8:      Convergence_1 = **FALSE**;
9:    **END IF**
10:   Given $\{\mathrm{p}_k(n)\}_{k=1}^{\Psi}$, solve (25)-(30) to get $\{t_j(n)\}_{\forall j \in \mathcal{Z}_{Z+1}}$;
11:   **IF** $(t_j(n) - t_j(n-1) \leq \epsilon)$ & $(n > 2)$
12:     Convergence_2 = **TRUE**;
13:     **RETURN** $t_j^\star = t_j(n-1)$, $\{\mathrm{p}_k^\star\}_{k=1}^{\Psi} = \{\mathrm{p}_k(n-1)\}_{k=1}^{\Psi}$;
14:   **ELSE**
15:     $t_j(n+1) = t_j(n)$, $\forall j$, and $n = n + 1$;
16:     Convergence_2 = **FALSE**;
17:   **END IF**
18: **UNTIL** Convergence_1 = **TRUE** & Convergence_2 = **TRUE**.

---

where t_j denotes the introduced intermediary slack-variable corresponding to the jth user, $\forall j \in \mathcal{Z}_{Z+1}$, with other parameters having same definitions as described previously. Note that the non-convex constraint of rank($\mathbf{W}_k$) = 1 is dropped as a part of standard SDR procedure. Since the objective function in $(P4)$ is an affine[5] (or concave) function and the constraint set is also convex, the modified optimization problem in $(P4)$ is in the standard form of a convex programming problem that can be solved by standard numerical methods such as the interior-point method [42]. It is obvious that joint optimization of the involved parameters ($\{\mathbf{W}_k\}_{k=1}^{\Psi}$ and $\{t_j\}_{\forall j \in \mathcal{Z}_{Z+1}}$) corresponding to $(C2) \cdots (C4)$ is difficult to realize using the CVX solver, in general. However, an iterative-based computation of parameters is possible to seek a suitable solution. Therefore, $(P4)$ can be successfully solved by the proposed convex programming based on an iterative method for maximization of harvested energy, as summarized in Algorithm 1. The pivotal stage for the proposed iterative method based solution is to develop an intermediate SVR-parameter update policy for solving the formulated problem. In order to understand the method behind the proposed alternating algorithm for harvested energy maximization, we subdivide it into two steps. In the first step (lines 3-9), we compute the precoder metrics $\{\mathbf{W}_k\}_{k=1}^{\Psi}$ for fixed values of $\{t_j\}_{\forall j \in \mathcal{Z}_{Z+1}}$, where any values are permissible, respectively, provided that $(P4)$ remains tractable. The corresponding optimized values of $\{\mathbf{W}_k\}_{k=1}^{\Psi}$ are then used in the second step of the algorithm (lines 10-17), where joint optimization of $\{t_j\}_{\forall j \in \mathcal{Z}_{Z+1}}$ is carried out. Upon the completion of the second step, the optimized values of $\{t_j\}_{\forall j \in \mathcal{Z}_{Z+1}}$ are fed again to the first step and this iterative process is repeated until the convergence of objective in $(P4)$. To proceed further, we propose the following proposition.

Proposition 2: For a given $\{t_j\}_{\forall j \in \mathcal{Z}_{Z+1}}$, *the objective function* (19) *is affine in* $\{\mathbf{W}_k\}_{k=1}^{\Psi}$.

Proof: From $(C2)$, and $(C3)$ of $(P4)$, it is clear that the objective is directly related to $\{\mathbf{W}_k\}_{k=1}^{\Psi}$. Therefore, each

iterative computation of $\{\mathbf{W}_k\}_{k=1}^{\Psi}$ corresponding to $(C4)$ would affect $\{t_j\}_{\forall j \in \mathcal{Z}_{Z+1}}$. Based on the nature of $(P4)$, it is obvious that the objective is an increasing affine function which attains the maximum when equality in $(C4)$ is reached. The proof is straightforward from this analytical reasoning. ∎

To prove the convergence of the proposed SVR-based solution, we first prove that the corresponding slack-variable metric, $\{t_j\}_{\forall j \in \mathcal{Z}_{Z+1}}$, increases in each iteration. Then, we prove that if the number of iterations is large enough, then the SVR-parameters $\{t_j\}_{\forall j \in \mathcal{Z}_{Z+1}}$ converge to the optimal $\{t_j^\star\}_{\forall j \in \mathcal{Z}_{Z+1}}$ such that the optimality condition in *Proposition 2* is satisfied, i.e., $\sum_{\forall j \in \mathcal{Z}_{Z+1}} t_j^\star = \sum_{\forall j \in \mathcal{Z}_{Z+1}} \mathcal{E}_j^{\mathcal{N}}(\mathbf{W}^\star)$. Let $\{\mathbf{W}_k(n)\}_{k=1}^{\Psi}$ denote the precoder metrics in the n-th iteration. Suppose $t_j(n) \neq t_j^\star$ and $t_j(n+1) \neq t_j^\star$, $\forall j \in \mathcal{Z}_{Z+1}$, represent the SVR-values in the iterations n and $n+1$, respectively. It is obvious from *Proposition 2* that $t_j(n) > 0$ and $t_j(n+1) > 0$ will hold and that $\sum_{\forall j \in \mathcal{Z}_{Z+1}} t_j(n+1) > \sum_{\forall j \in \mathcal{Z}_{Z+1}} t_j(n)$. Therefore, we can show that as long as the number of iterations is large enough, $\sum_{\forall j \in \mathcal{Z}_{Z+1}} t_j(n)$ will eventually approach the maximum and satisfy the optimality condition as stated in *Proposition 1*. However, the global optimality of the solution may not be guaranteed due to prior constraint relaxation according to SDR.

B. Power-Refinement Process

We observe that the solution obtained for $(P4)$ via CVX yields similar outcomes like the ones attained in the previous section. The JMEP and PIEP achieve rank-1 solutions for most of the experiments, however this outcome is not certain in general. The solutions corresponding to SMEP are indeed rank-1 for the MC group precoders, while multi-rank solutions are achieved for last group (with EH users). Again, this implicates that Z MC precoders would easily serve the ID users and the EH users will be aided with the help of rank($\mathbf{W}_{Z+1}$) precoders. From a hardware implementation perspective, such sub-optimal solution makes it difficult to ensure the practical tractability of SMEP system. Therefore, the Gaussian randomization technique [12] is employed to curtail the multi-ranked $\{\mathbf{W}_{Z+1}\}$ into a unit rank, which

---

[5]Note that the sum of affine functions is an affine function. Additionally, an affine function is both convex as well as concave in nature [36]. Herein, it may be claimed that we tackle maximization of a concave function.

in-turn induces additional computational complexities. In order to ensure the optimality condition in *Proposition 2*, we first compute the individual directions using the eigen value decomposition (EVD) [40] or randomization technique (as above) [12] for Z MC precoders and use the randomization method for the precoder corresponding to $\{\mathbf{W}_{Z+1}\}$. Then, the vector indicating the direction of kth precoder is given by $\widetilde{\mathbf{w}}_k = \frac{\mathbf{w}_k}{||\mathbf{w}_k||_2}$. We reformulate $(P4)$ and obtain the problem $(P5)$, as follows

$$(P5): \max_{\substack{\{\mathrm{p}_k\}_{k=1}^{\Psi} \\ \{t_j\}_{\forall j \in \mathcal{Z}_{Z+1}}}} \sum_{\forall j \in \mathcal{Z}_{Z+1}} t_j \qquad (25)$$

$$\text{s.t.} \quad (C1): |\widetilde{\mathbf{w}}_k^H \mathbf{g}_i|^2 \mathrm{p}_k - \gamma_i \sum_{\ell \neq k} |\widetilde{\mathbf{w}}_\ell^H \mathbf{g}_i|^2 \mathrm{p}_\ell$$

$$\geq \gamma_i(\sigma_{R,i}^2 + \sigma_{D,i}^2),$$

$$\begin{cases} \text{SMEP}: & \forall i \in \mathcal{Z}_k, \ \forall k \in \{1,\dots,Z\}, \\ & \forall \ell \in \{1,\dots,Z+1\}, \\ \text{JMEP}: & \forall i \in \mathcal{Z}_k, \ \forall k \in \{1,\dots,Z\}, \quad (26) \\ & \forall \ell \in \{1,\dots,Z\}, \\ \text{PIEP}: & \forall i, \forall k, \forall \ell \in \{1,\dots,K\}, i=k, \end{cases}$$

$$(C2): \frac{1}{1 + e^{(-\alpha(\sum_{k=1}^{\Psi} |\widetilde{\mathbf{w}}_k^H \mathbf{g}_j|^2 \mathrm{p}_k) + \alpha\beta)}}$$

$$\geq t_j \left(\frac{1-\phi}{\mathcal{E}'}\right) + \phi, \quad \forall j \in \mathcal{Z}_{Z+1}, \quad (27)$$

$$(C3): t_j \geq \xi_j, \quad \forall j \in \mathcal{Z}_{Z+1}, \qquad (28)$$

$$(C4): \sum_{k=1}^{\Psi} \mathrm{p}_k \leq \mathrm{P}_{\text{Max}}, \qquad (29)$$

$$(C5): \mathrm{p}_k \geq 0, \qquad (30)$$

where p_k is the power term associated to the kth precoder with $\widetilde{\mathbf{w}}_k$ as its direction, and other terms have the same meaning as defined previously. In other words, the scalar p_k is optimized in the direction of $\widetilde{\mathbf{w}}_k$. Thereafter, the solution to $(P5)$ can be obtained directly using the CVX solver, which is summarized in Algorithm 2. Consequently, Directional Power Maximization Algorithm (DPMA) ensures that the optimality condition in *Proposition 2* is always satisfied with rank-1 solutions for all precoders. Consequently, the proof of convergence of Algorithm 2 would follow the same process as presented in the previous section. From the programming viewpoint, the convergence of Algorithm 1 and Algorithm 2 could be determined by setting an extremely low threshold value (say ϵ), such that the stopping criteria is defined by $\sum_{\forall j \in \mathcal{Z}_{Z+1}} t_j(n+1) - \sum_{\forall j \in \mathcal{Z}_{Z+1}} t_j(n) \leq \epsilon$.

C. Computational Complexity Analysis

Suppose that the CVX solver incurs the computational complexities of $\kappa_1(\Psi, M)$ orders for carrying out the operations 4: to 9:, and $\kappa_2(M)$ orders to process 11: to 17:, respectively, corresponding to Algorithm 1, and linear orders for Algorithm 2. Consequently, the overall computation complexities for SMEP, JMEP, and PIEP are respectively

$$\mathcal{O}\left(\left((K^5 \cdot N^3 \cdot (N-1)^2)^{\left(\kappa_1(Z+1,M)+\kappa_2(M)\right)}\right)^{\chi(n,\gamma_i,\xi_i)}\right),$$

$$\mathcal{O}\left(\left((K^5 \cdot (N-1)^6)^{\left(\kappa_1(Z,M)+\kappa_2(M)\right)}\right)^{\chi(n,\gamma_i,\xi_i)}\right), \text{ and}$$

$$\mathcal{O}\left(\left((K^7 \cdot (N-1)^2)^{\left(\kappa_1(K,M)+\kappa_2(M)\right)}\right)^{\chi(n,\gamma_i,\xi_i)}\right), \text{ where}$$

$\chi(n, \gamma_i, \xi_i)$ denotes the factor dependent on n iterations of algorithm(s), γ_i and ξ_i, corresponding to each of the respective scenarios. We demonstrate the effectiveness of proposed methods in the following section.

V. SIMULATION RESULTS

In this section, we present a comparative study between SMEP, JMEP and PIEP. The three cases viz-a-viz., SMEP, JMEP, and PIEP are implemented using MATLAB R2017a, with optimization performed via convex programming tool CVX [37], [38], and the solutions obtained with the help of SEDUMI solver.

A. Simulation Environment

We assume an ITU-R indoor model (2-floor office scenario) [43] to generate channel realizations with the path-loss exponent given by

$$\text{PL (in dB)} = 20 \log_{10}(F) + N \log_{10}(D) + P_f(n) - 28, \quad (31)$$

where F is the operational frequency (in MHz), N is the distance power loss coefficient, D is the separation distance (in metres) between the transmitter and end-user(s) (with $D > 1$m), $P_f(n) = 15 + 4 (n\text{-}1)$ is the floor penetration loss factor (in dB), and n is the number of floors between the transmitter and the end-user(s) (with $n \geq 0$). Specifically, the chosen parametric values are F = 2.4 GHz, D is randomly chosen between 4m and 5m (unless specified otherwise), N = 30, and $P_f(2)$ = 19 dB. It is noteworthy that the channel state information (CSI) will not be affected largely, due to the assumption of an indoor scenario . Moreover, the CSI loops within the coherence time of the channel where the dynamic nature in CSI may be assumed to be introduced from the environment as well as user mobility in some way [43]. In this context, wider beam widths could be desirable from a signal reception point of view (due to mobility), while narrow beams might be better to control the interference.

The transmitter is assumed to be equipped with M = 20 antennas (unless specified otherwise), while K = 10 users are distributed within $(Z+1)$ = 5 groups as follows: $\mathcal{Z}_1 = \{U_1, U_3, U_4\}$, $\mathcal{Z}_2 = \{U_2, U_5\}$, $\mathcal{Z}_3 = \{U_6, U_8\}$, $\mathcal{Z}_4 = \{U_7, U_9, U_{10}\}$, and $\mathcal{Z}_5 = \{U_1, U_5, U_8, U_{10}\}$, where $\mathcal{Z}_5$ is the EH group of users while the remaining $(\mathcal{Z}_1, \dots, \mathcal{Z}_4)$ MC groups are comprised of ID users. We set $\sigma_{R,i}^2$ = -110 dBW, $\sigma_{D,i}^2$ = -80 dBW and ζ_i = 0.6. Furthermore, an average of 500 random channel realizations (with random placement of end-users in every realization) is presented for each experiment corresponding to the transmit power minimization problem, while an average of 100 experiments is performed to analyze the harvested energy maximization problem. The constants corresponding to the non-linear EH circuit are chosen as $\mathcal{E}'$ = 2.8 mJ, α = 1500, and β = 0.0022 [33], [34].
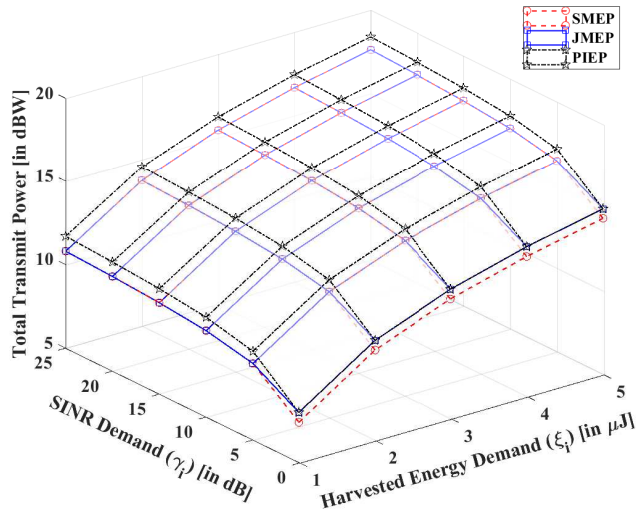
Fig. 5. Performance analysis of SMEP, JMEP and PIEP in terms of total transmit power versus the harvested energy demands and the SINR demands of users where $D = 5$m and $M = 20$.
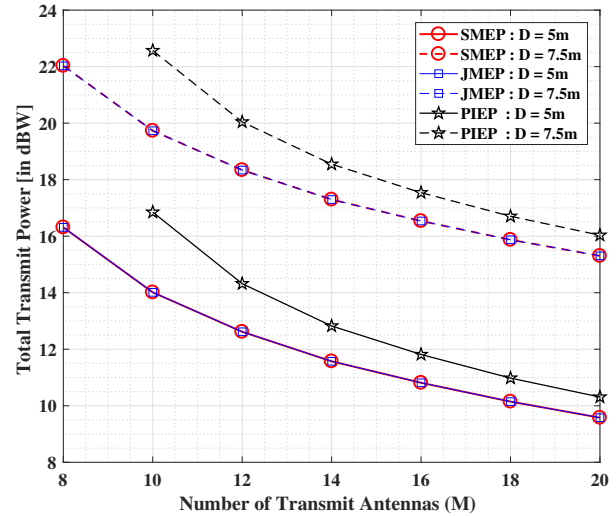

Fig. 6. Performance analysis of SMEP, JMEP and PIEP in terms of total transmit power versus the number of transmit antennas with variation in distance where $\gamma_i = 5$ dB and $\xi_i = 1$ μJ.

B. Discussion on Optimization Solutions

Before we provide detailed discussion on the optimization solutions, it is important to highlight the challenges related to the adoption of considered non-linear EH model in comparison to a linear EH scheme. Due to the introduction of a non-linear (exponential) function to characterize the EH operation, the traditional equations and definitions with linear form require alteration accordingly. With regard to the optimization problems, incorporation of the non-linear EH model leads to intractability which requires rigorous transformations and relaxations in comparison to the case with the linear EH model. Moreover, several challenges are encountered while seeking suitable solution(s) in this context. Specifically, the problems require adequate transformations to be solved by the convex optimization solvers (e.g., we use the CVX in this work, which requires a particular form of input problem formulation).

It has been shown in [44] that a solution pertaining to rank$(\mathbf{W}_k^\star) = 2$ can still be viewed as optimal. Furthermore, it can be reduced to rank$(\mathbf{W}_k^\star) = 1$ at an additional computation cost thereby penalizing the system performance and increasing the chance that not all constraints will be satisfied. Therefore, we consider the rank$(\mathbf{W}_k^\star) \leq 2$ solution as optimal. In other cases, i.e., for rank$(\mathbf{W}_k^\star) > 2$, the solution is considered sub-optimal with further scope of improvement.

In the context of both the energy optimization problems, i.e., total transmit power minimization (in $(P1)$) and sum-harvested energy maximization (in $(P3)$), it is found that the solutions of both JMEP and PIEP are indeed rank-1 for most of the experiments whereas such an outcome cannot be assured to be always true, in general. The solution corresponding to SMEP is found to be unit rank for lower values of SINR and harvested energy demands. Further, this effect seems to vanish with higher demands of SINR and harvested energy where multi-rank solutions are obtained for the last group (harvested

energy serving precoders). One interpretation of multi-rank solution obtained for $\{\mathbf{W}_{Z+1}\}$ corresponding to the EH group implies that in order to serve EH specific users, more precoders $(Z'$ in number(s), with $Z' = $ rank$(\mathbf{W}_{Z+1}))$ would be required. The ID users are served using the beams of corresponding Z MC precoders while the EH users utilize rank$(\mathbf{W}_{Z+1})$ precoders for collecting energy, which is sub-optimal and difficult to implement from a hardware perspective. Therefore, the randomization technique [12] is implemented to reduce the multi-rank solution for $\{\mathbf{W}_{Z+1}\}$ to a unit rank thereby introducing additional computational penalties while ensuring tractability in terms of hardware implementation. Another interpretation that the multi-rank solution suggests is to split the EH group into multiple groups, so that the energy can be better focused across the respective group channel vectors. However, it is noteworthy that the presence of energy-specific precoder for last group becomes redundant for very high demands of SINR, where SMEP is found to yield similar performance as JMEP. Regarding the realization of algorithms in practical systems, offloading may be performed where the computation task is carried out by a centralized node [45], [46]. In this context, adequate signaling or feedback mechanism may be utilized by the central controller to inform the concerned nodes.

C. Numerical Analysis

In Fig. 5, we illustrate the effect on the total transmit power (in dBW) with increasing demand of the harvested energy and the SINR threshold. Performance benefits of the proposed SMEP are seen over JMEP and PIEP, where SMEP is observed to perform best at low SINR and/or EH demands. Apparently, JMEP encounters a contradictory SINR-EH demand constraint at lower values of SINR demand which makes it difficult to attain optimal precoder designs. However, it is clear that the performance of SMEP and JMEP would converge together at
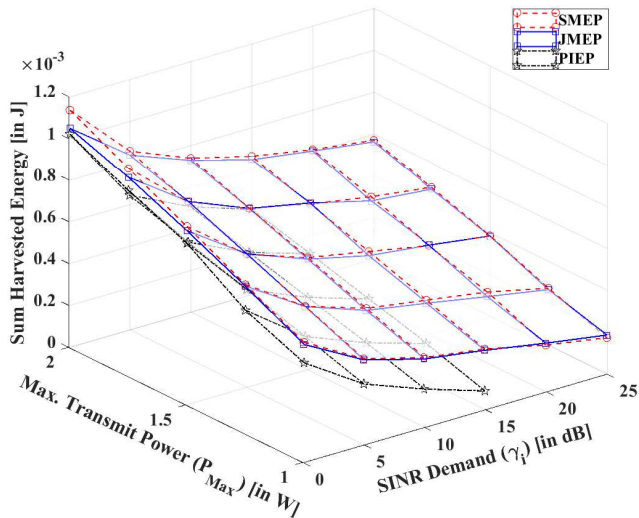
Fig. 7. Performance analysis of SMEP, JMEP and PIEP in terms of sum-harvested energy versus the maximum transmit power limits and variation in the SINR of users with $\xi_i = 10$ nJ.
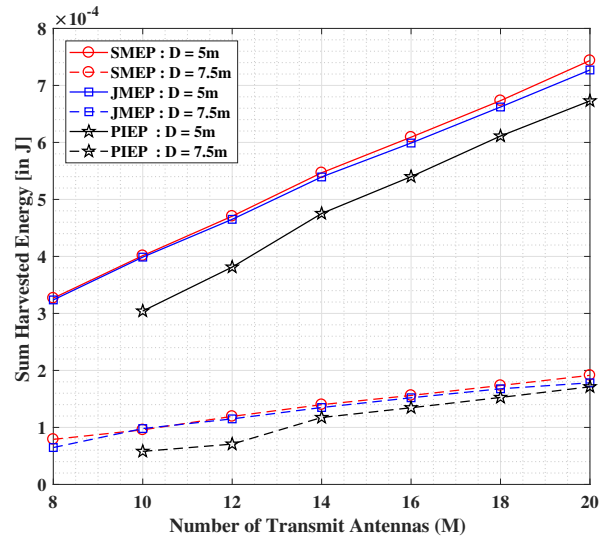

Fig. 8. Performance analysis of SMEP, JMEP and PIEP in terms of sum harvested energy versus the number of transmit antennas with variation in distance where $\gamma_i = 1$ dB, $\xi_i = 1$ nJ and $P_{Max} = 1.5$ W.

higher SINR demand, where the contribution from energy-dedicated precoder in SMEP can be considered negligible. It is needless to mention that SMEP can successfully take care of distinct user types without any complications, while JMEP would require additional computation to categorize the EH users within the intended Z groups to ensure its efficient performance. In general, the total transmit power increases with higher demands of SINR and/or EH thresholds for all the three cases viz-a-viz., SMEP, JMEP, and PIEP.

Fig. 6 shows the variation in total transmit power (in dBW) with increasing number of array antennas at the transmitter for $\gamma_i = 5$ dB and $\xi_i = 1$ μJ. Herein, we compare the proposed SMEP with the two benchmarks JMEP and PIEP, respectively. It is observed that the system performance for all the scenarios improves considerably in terms of the total transmit power with increasing number of transmit array antennas, where SMEP is seen to perform the same as JMEP, while both SMEP and JMEP outperforms PIEP. Furthermore, a similar trend is observed when the distance between the transmitter and end-users is increased with the placement in between $D = 6.5$m and $D = 7.5$m. However, an expected increase in the total transmit power is also observed in this case. It is also noteworthy that JMEP and SMEP are operational even with lower number of transmit array antennas in comparison to the number of end-users while the former (number of transmit array antennas) should be equal or greater than the latter (number of end-users) to ensure operability of PIEP.

Considering the case where the impact on the scenarios with respect to the number of users, it is noteworthy that the SINR and EH demands in Fig. 5 may be synonymously translated into the number of users. In simple terms, this duality with more number of users would correspond to high SINR and EH demands and vice-versa. It is observed that the total transmit power increases or decreases with the increase or decrease in number of users, respectively. Regarding the number of

antennas, it is observed from Fig. 6 that increasing number of antennas would facilitate the users with optimized transmit power at the the precoders. Therefore, similar trend should be observed as above, where more number of antennas would be beneficial in terms of improving the system performance(s).

In Fig. 7, we present the impact on the sum-harvested energy (in Joules) with increasing SINR threshold and maximum power limitations with $\xi_i = 10$ nJ. The objective increases with rising values of maximum transmit power limitations while it is seen to decrease with growing SINR demands for all the three scenarios namely SMEP, JMEP and PIEP. Both SMEP and JMEP are found to provide superior performances over PIEP, with SMEP operating nearly same as JMEP at lower P_{Max} values and higher SINR demands. However, the efficiency of SMEP is significantly higher than JMEP at higher values of P_{Max} and SINR demands. In addition, PIEP is found to approach an infeasible regime at higher values of SINR demands (for most of the experiments) and thus the results appear to terminate at $\gamma_i = 15$ dB. Moreover, it is noteworthy that the working characteristic of SMEP is naturally viable to take care of separate information and/or energy users more competently in comparison to JMEP and PIEP, with a remarkable performance.

Fig. 8 depicts the variation in sum-harvested energy (in Joules) with increasing number of transmit antenna arrays with $\gamma_i = 1$ dB, $\xi_i = 1$ nJ and $P_{Max} = 1.5$ W. It is seen that SMEP provides better performance in comparison to JMEP and PIEP, where the objective increases appreciably with growing number of antennas. Similar trend is observed when the designated users are placed randomly between $D = 6.5$m and $D = 7.5$m, from the ULA-equipped transmitter. As noticed previously, SMEP and JMEP are functional even at lower number of antennas in comparison to the number of users, while the minimum number of antennas should atleast be same as the number of users for PIEP to be operational.
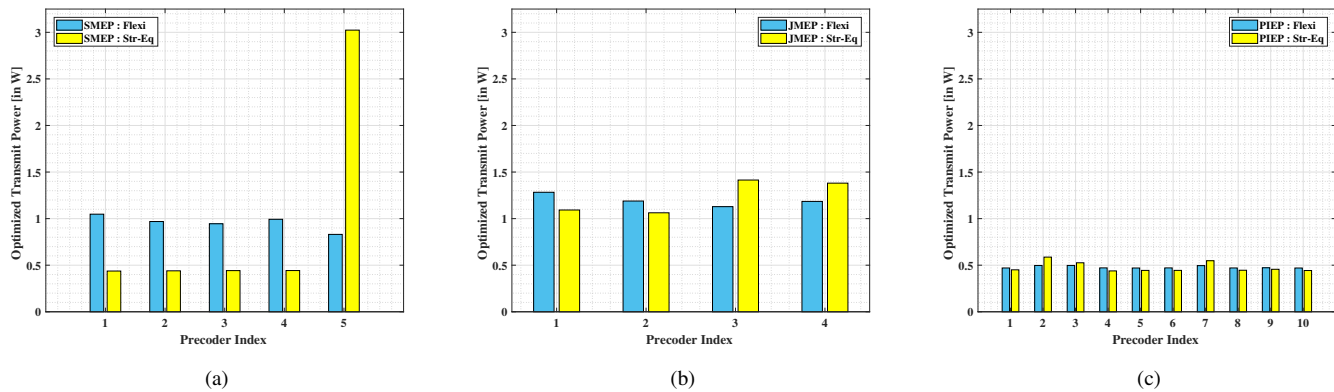
Fig. 9. Optimized transmit power of the precoders following the total transmit power minimization problem for (a) SMEP, (b) JMEP and (c) PIEP.
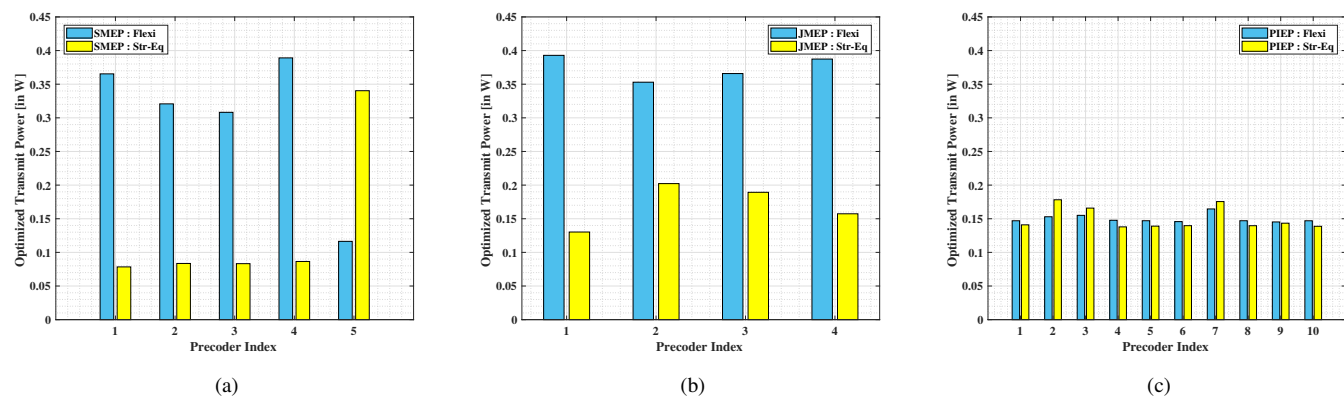

Fig. 10. Optimized transmit power of the precoders following the sum-harvested energy maximization problem for (a) SMEP, (b) JMEP and (c) PIEP.

In this direction, it is important to discuss about the system performance with varying number of users. As mentioned previously, the duality between the user demands and the number of users may be assumed. In this regard, the results from Fig. 7 indicate that for a fixed number of transmit antennas, the sum-harvested energy would decrease or increase with growing or depreciating number of users (synonymous with SINR and EH demands). Whereas, the results in Fig. 8 shows the benefits of increasing the number of antennas on system performance under a specific transmit power limitation. Moreover, the number of heterogeneous user types and their placement would also affect the overall performance corresponding to the maximization of sum-harvested energy by the intended users.

Next, we set $\gamma_i = 0.1$ dB, $\xi_i = 1$ μJ in Fig. 9 and $\gamma_i = 0.1$ dB, $\xi_i = 1$ nJ and $P_{\text{Max}} = 1.5$ W in Fig. 10, and consider any random realization of $\mathbf{g}_i$, to investigate the effectiveness of the exclusive precoder in SMEP designated to serve the group of EH users in comparison to the JMEP and PIEP scenarios, corresponding to the two energy optimization problems in (6) and (13), respectively. Herein, we consider two experiments to study the problems on energy optimization more keenly. In the first test, we assume that the inequality in the SINR constraint i.e., $(C1)$ of all the formulated problems $(P1) \cdots (P5)$ holds; which we refer to as the flexible (Flexi) form of the

problem since there is no hard boundation on the computed SINR and each user may obtain equal to or more than the demanded SINR threshold. Whereas in the other (second) test, we consider that a strict equality (Str-Eq) holds in $(C1)$ of $(P1) \cdots (P5)$, meaning that each user will be provided neither more nor less, but equal to the exact SINR demand. Before we proceed, it is important to mention that all the prior simulation results were obtained via first experiment trial (which is more general from practical perspective). From our previous observations in the performance analysis of SMEP, JMEP and PIEP, we find that the main investigation lies in the low SINR demand regime, where the impact of the precoder for energy group in SMEP is maximum.

Considering the total transmit power minimization problem, we show in Fig. 9 the comparison between the three considered schemes namely, SMEP, JMEP and PIEP. As discussed above, we perform the evaluation over the two experiments viz., Flexi and Str-Eq. The significance of the exclusive precoder in SMEP corresponding to the group of EH users is explicitly visible (with reference to Precoder Index = 5) in Fig. 9(a), when compared with JMEP in Fig. 9(b) and PIEP in Fig. 9(c). From the outcomes of the two experiments in all cases, we find that the exclusive precoder in SMEP corresponding to the group of EH users becomes more significant in terms of reducing the complexity in power allocations at the stipulated precoders.
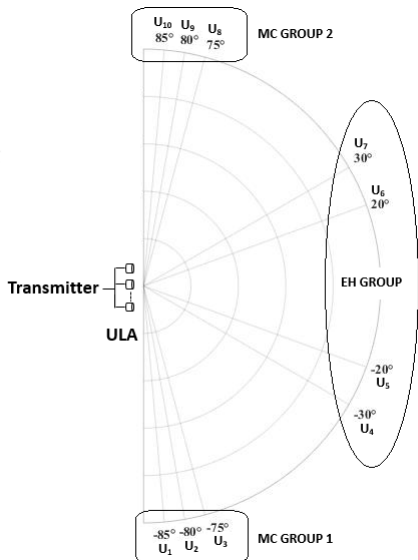
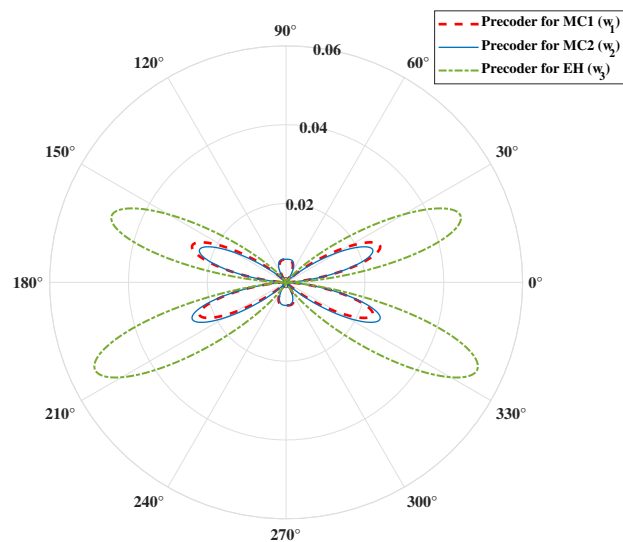Fig. 11. User placing within groups, served via ULA-equipped transmitter.

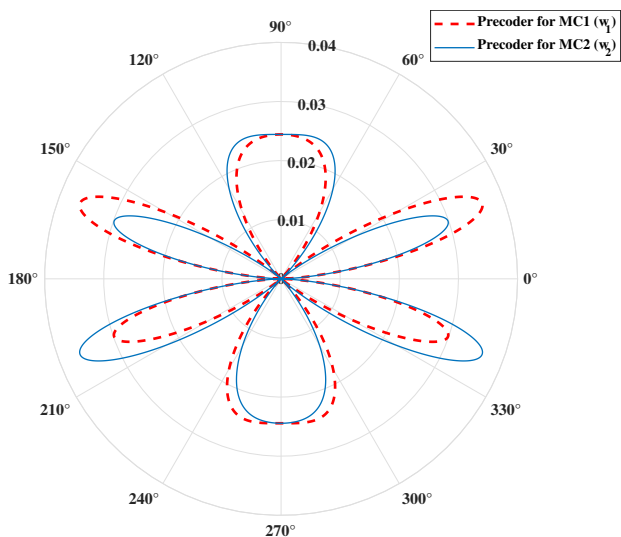Fig. 13. Antenna radiation beam pattern for SMEP.
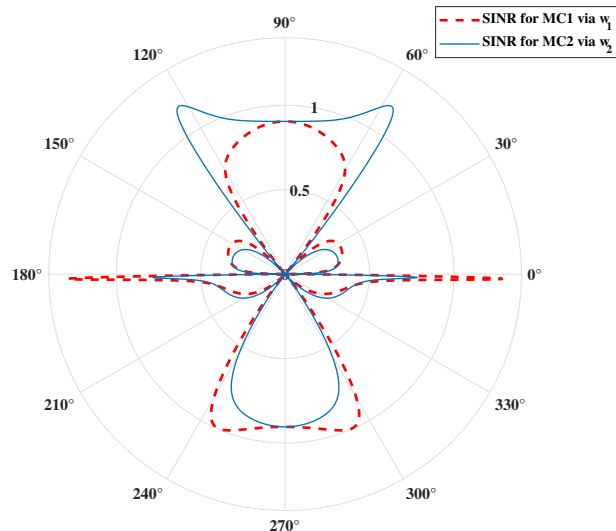

Fig. 12. Antenna radiation beam pattern for JMEP.

Fig. 14. SINR pattern of MC precoders in SMEP.

Whereas the other systems (JMEP and PIEP) require more transmit power to take care of the contradictory constraints of low SINR and high EH demands at the corresponding users.

In Fig. 10, we consider the problem of sum-harvested energy to illustrate the comparison between SMEP (in Fig. 10(a)), JMEP (in Fig. 10(b)) and PIEP (in Fig. 10(c)) for a fixed maximum transmit power limitation of P_{Max} = 1.5 W. The results are obtained after the two experiments (Flexi and Str-Eq., respectively), are performed for the aforementioned three schemes. Herein, we observe similar outcomes like in the above-mentioned analysis, indicating the benefits of adopting an exclusive precoder in SMEP for the group of EH users, over JMEP and PIEP schemes in the low SINR and high EH demand regimes.

D. Further Investigation via Uniform Linear Arrays

In this section, we consider a more generalized line-of-sight (LoS)-based channel model in comparison to the previous cases, for investigating the performances of SMEP and JMEP further. Herein, we assume a scenario similar to 802.11 frameworks [47] (e.g., 802.11b), where the bandwidth is considered to be 20 MHz with an operational frequency of 2.4 GHz. A uniform linear arrays (ULAs)-based transmitter is presumed for investigating the proposed methods in a practically motivated environment. Please note that in this case, an antenna gain of 10 dB is also taken into consideration, along with (31). The corresponding $M \times 1$ complex vectors indicating the phase shift from each element of transmit antenna array to the receive antenna of ith user, where $i \in \{1, \ldots, K\}$, are

Vandermonde

$$\mathbf{v}(\varphi_i) = [1 \quad e^{j\varphi_i} \quad e^{j2\varphi_i} \quad \dots \quad e^{j(M-1)\varphi_i}]^T, \qquad (32)$$

where $\varphi_i = -2\pi d \sin(\theta_i)/\lambda$, and $j = \sqrt{-1}$. Herein, d denotes the spacing between successive antenna elements, λ is the carrier wavelength, and the angles θ_i (in radians) define the direction of the ith user from the transmitter. Assume $\boldsymbol{\rho}_i$ as the $M \times 1$ scalar vector indicating the path loss from M transmit (ULA) antennas to the ith user modeled according to (31). Then, the equivalent channel vector for the ith user is given by $\mathbf{g}_i = \mathbf{v}(\varphi_i) \odot \boldsymbol{\rho}_i$, where $\odot$ denotes the Hadamard product. Note that the phase orientation of ULA set-up must be unaffected due to this operation.

The transmitter is assumed to be equipped with $M = 4$ antennas (unless specified otherwise) spaced $d = \lambda/2$ apart, while $K = 10$ users are distributed within $(Z + 1) = 3$ groups as follows: $\mathcal{Z}_1 = \{U_1(-85°), U_2(-80°), U_3(-75°)\}$, $\mathcal{Z}_2 = \{U_8(75°), U_9(80°), U_{10}(85°)\}$, $\mathcal{Z}_3 = \{U_4(-30°), U_5(-20°), U_6(20°), U_7(30°)\}$, where $\mathcal{Z}_3$ is the EH group of users while the remaining $(\mathcal{Z}_1, \mathcal{Z}_2)$ MC groups are comprised of ID users. Note that $U_i(\theta_i)$ denotes the angular placement of ith user at an angle θ_i from the ULA. This arrangement is depicted in Fig. 11 for better visual understanding. Further, we perform the numerical evaluation corresponding to the sum-harvested maximization problem in $(P3)$ for SMEP and JMEP, wherein we assume $\mathrm{P_{Max}} = 0.1$ W, $\gamma_i = 0.2$ dB[6], and $\xi_i = 1$ nJ.

For further analysis, the ULA radiation beam-pattern for each precoder is obtained by using the sum of transmit power via corresponding precoder in all the directions between $[-\pi, \pi]$ radians. Specifically, the radiation beam-pattern for k^{th} precoder is defined as $\sum_{\forall \varphi_i} \mathbf{w}_k^H \mathbf{v}(\varphi_i)$, where $\varphi_i = -2\pi d \sin(\theta_i)/\lambda$, with $\theta_i \in [-\pi, \pi]$. Similarly, the SINR pattern for k^{th} MC precoder is expressed by $\sum_{\forall \varphi_i} \mathbf{w}_k^H \mathbf{v}(\varphi_i) / \sum_{\substack{\ell=1 \\ \ell \neq k}}^{\Psi} \sum_{\forall \varphi_i} \mathbf{w}_\ell^H \mathbf{v}(\varphi_i)$, where $\varphi_i = -2\pi d \sin(\theta_i)/\lambda$, with $\theta_i \in [-\pi, \pi]$.

In Fig. 12, the ULA radiation beam-pattern is depicted using the SDR-based precoder solutions of the considered sum-harvested maximization in JMEP. It is observed that the two designated precoders fulfill the information and energy demands of the users in distinct groups. Similarly, we depict in Fig. 13 the ULA radiation beam-pattern for the above-mentioned problem considering the case of SMEP. It is seen that the precoder corresponding to the EH group of users meets their demands via exclusively designed beams, with slight assistance from the other two MC-specific precoders, as expected. Such a case emphasizes on the need of separate waveform designs for ID and EH operations for further improvement in system efficiency [31]. Next, we show the SINR-based beam patterns in Fig. 14, for the same case of SMEP. The operations of the two dedicated precoders for MC groups are presented, wherein they provide the requested SINR demands at the MC groups. As anticipated (with the help of observations in prior section), SMEP is found to perform better than JMEP, specifically with $\left(\sum_{\forall j \in \mathcal{Z}_{Z+1}} \mathcal{E}_j^{\mathcal{N}}\right)_{\text{SMEP}} =$

5.4403 μJ and $\left(\sum_{\forall j \in \mathcal{Z}_{Z+1}} \mathcal{E}_j^{\mathcal{N}}\right)_{\text{JMEP}} = 4.3615$ μJ, respectively, for the presented ULA-based results.

E. Summary

The overall outcomes imply that the solutions for JMEP and PIEP are (locally) optimal while (local) sub-optimal results are obtained for SMEP, which are rectified with the help of Gaussian randomization approach. From the hardware implementation perspective, this means that even with additional precoder(s) in comparison to JMEP, SMEP is seen to provide relatively better performance. However, both SMEP and JMEP provide comparably similar performance at higher demands of SINR implying that enough power could be harvested from the corresponding SINR beams and that the last group's energy precoder becomes redundant in case of SMEP[7]. *It is important to highlight that the adoption of separate precoder designs for ID and EH operations does not only reduce the complexity at the transmit source, but also improves the overall system performance both in terms of transmit power minimization as well as maximization of sum-harvested energy. Besides, the proposed JMEP method may be considered a special case or a sub-system of SMEP. Moreover, SMEP has another advantage where its flexibility may facilitate the adoption of different waveform designs, for the ID and EH operations, respectively. In this regard, recent studies, e.g., [31], have shown that the structure of the two waveforms can be rather different.* The operation of PIEP involves same number of precoders as the users, which is good for individual users but it naturally imposes an overall high power consumption, thereby imposing large computational complexities. Moreover, PIEP may even fail to provide the minimum (high) demands of SINR and EH demands at relevant users due to insufficient transmit power in case of sum-harvested energy maximization of the corresponding users.

VI. CONCLUSION

We considered precoding in multi-group multicast system(s) to guarantee the coexistence of three wireless user types, respectively capable of information decoding only, energy harvesting only, and information decoding and/or energy harvesting. In this context, two problems were formulated to minimize the total transmit power, and to maximize the overall harvested energy, respectively; both subjected to the constraints on minimum SINR and EH demands at the corresponding users. The aforementioned problems were transformed with the use of semidefinite relaxation technique considering three scenarios, namely, Separate Multicast and Energy Precoding Design (SMEP), Joint Multicast and Energy Precoding Design (JMEP), and Per-User Information and/or Energy Precoding Design (PIEP), respectively. Moreover, an additional slack variable reduction method was adopted to make the harvested energy maximization problem tractable. Suitable solutions with considerably good performance were proposed to address the aforementioned problems. Performance benefits of SMEP

---

[6]This demand enables the provision of data speeds same or higher than 5 Mbps at each user, which is sufficient for HD quality video streaming [48].

[7]It is worth mentioning that the case with contradictory constraints of low SINR and high EH demands is also difficult to realize in the JMEP scenario.

were shown over JMEP and PIEP, in terms of handling low-SINR user demands with no additional computational task for categorizing the EH users, unlike its sub-system counterpart, JMEP. This motivates the adoption of SMEP in practical cases. This work can be extended to several interesting directions, such as the analysis of the proposed framework with alternative low-complexity based techniques, investigation of the optimization problems with optimized grouping techniques, consideration of MIMO systems, and further analysis with massive MIMO.

APPENDIX A
CONVERSION OF NON-LINEAR ENERGY HARVESTING CONSTRAINT TO LINEAR CONSTRAINT

The non-linear EH constraint at the ith user is given by

$$\frac{\mathcal{E}'}{1-\phi} \cdot \left(\frac{1}{1 + e^{(-\alpha(\sum_{k=1}^{\psi} |\mathbf{w}_k^H \mathbf{g}_i|^2) + \alpha\beta)}} - \phi \right) \geq \xi_i, \quad (33)$$

where ξ_i is the harvested energy demand at the ith user.

The expression in (33) can be re-arranged and written as

$$\frac{\mathcal{E}'}{1-\phi} \cdot \left(\frac{1}{1 + e^{(-\alpha\mathcal{E}_i^{\mathcal{L}}/\zeta_i + \alpha\sigma_{R,i}^2 + \alpha\beta)}} - \phi \right) \geq \xi_i. \quad (34)$$

Further simplification of (34) leads to the equivalent linear EH constraint

$$\mathcal{E}_i^{\mathcal{L}} \geq \xi_i', \quad (35)$$

where

$$\xi_i' = \zeta_i \left(\sigma_{R,i}^2 + \beta - \frac{1}{\alpha} \ln \left(\frac{(1-\phi)(\mathcal{E}' - \xi_i)}{(1-\phi)\mathcal{E}' + \phi\xi_i} \right) \right). \quad (36)$$

From (36), it is clear that ξ_i' is an up-scaled version of ξ_i and that the constraints in (8) and (33) are equivalent. QED. ∎

APPENDIX B
PROOF OF PROPOSITION 1

Consider the following expression, synonymous to the sub-term of (5),

$$F(x) = \frac{1}{1 + \exp(-ax + b)}. \quad (37)$$

It is clear that the optimization of $\mathcal{E}_j^{\mathcal{N}}(\mathbf{w})$ with respect to $\mathbf{w}$ would affect only the sub-term of (5), as represented in (37). Therefore, in order to understand the nature of $F(x)$, we express the first and second order derivative of the function with respect to x, respectively, as follows

$$\frac{\partial F(x)}{\partial x} = \frac{a \exp(-ax + b)}{(1 + \exp(-ax + b))^2}, \quad (38)$$

$$\frac{\partial^2 F(x)}{\partial x^2} = \frac{-a^2 \exp(-ax + b)(1 - (\exp(-ax + b))^2)}{(1 + \exp(-ax + b))^4}. \quad (39)$$

The parameters a and b may assume any value defined in [33], corresponding to the received input power (x) in the μW regime. Based on these parameter selections, it is explicit that $0 < \exp(-ax + b) < 1$. Therefore we have,

$$\frac{\partial^2 F(x)}{\partial x^2} < 0, \quad (40)$$

which implies that the $F(x)$ is a concave function within the specified limits of a, b and x. Hence proved. ∎

REFERENCES

[1] Q. Shi, L. Liu, W. Xu, and R. Zhang, "Joint Transmit Beamforming and Receive Power Splitting for MISO SWIPT Systems," *IEEE Trans. Wireless Commun.*, vol. 13, no. 6, pp. 3269–3280, June 2014.

[2] S. Gautam and P. Ubaidulla, "Relay Selection and Transceiver Design for Joint Wireless Information and Energy Transfer in Cooperative Networks," in *85th Veh. Tech. Conf. (Spring)*. IEEE, 2017, pp. 1–5.

[3] D. Mishra, G. C. Alexandropoulos, and S. De, "Harvested Power Fairness Optimization in MISO SWIPT Multicasting IoT with Individual Constraints," in *IEEE International Conference on Communications (ICC)*, May 2018, pp. 1–6.

[4] S. Gautam, T. X. Vu, S. Chatzinotas, and B. Ottersten, "Joint wireless information and energy transfer in cache-assisted relaying systems," in *IEEE Wireless Communications and Networking Conference (WCNC)*, April 2018, pp. 1–6.

[5] S. Gautam, T. X. Vu, S. Chatzinotas, and B. Ottersten, "Cache-Aided Simultaneous Wireless Information and Power Transfer (SWIPT) With Relay Selection," *IEEE J. Sel. Areas Commun.*, vol. 37, no. 1, pp. 187–201, Jan 2019.

[6] M. Sivakumaran and P. Iacopino, "The Mobile Economy 2018," https://www.gsma.com/mobileeconomy/wp-content/uploads/2018/05/The-Mobile-Economy-2018.pdf, 2018.

[7] R. Tandon, S. A. Jafar, S. Shamai, and H. V. Poor, "On the Synergistic Benefits of Alternating CSIT for the MISO Broadcast Channel," *IEEE Trans. Inf. Theory*, vol. 59, no. 7, pp. 4106–4128, July 2013.

[8] L. R. Varshney, "Transporting information and energy simultaneously," in *IEEE International Symposium on Information Theory*, July 2008, pp. 1612–1616.

[9] M. R. A. Khandaker and K. Wong, "SWIPT in MISO Multicasting Systems," *IEEE Wireless Commun. Lett.*, vol. 3, no. 3, pp. 277–280, June 2014.

[10] T. D. P. Perera, D. N. K. Jayakody, S. K. Sharma, S. Chatzinotas, and J. Li, "Simultaneous Wireless Information and Power Transfer (SWIPT): Recent Advances and Future Challenges," *IEEE Commun. Surveys Tuts.*, vol. 20, no. 1, pp. 264–302, Firstquarter 2018.

[11] Z. Ding, C. Zhong, D. W. K. Ng, M. Peng, H. A. Suraweera, R. Schober, and H. V. Poor, "Application of smart antenna technologies in simultaneous wireless information and power transfer," *IEEE Comm. Mag.*, vol. 53, no. 4, pp. 86–93, April 2015.

[12] N. D. Sidiropoulos and T. N. Davidson and, "Transmit beamforming for physical-layer multicasting," *IEEE Trans. Signal Process.*, vol. 54, no. 6, pp. 2239–2251, June 2006.

[13] Q. Shi, C. Peng, W. Xu, M. Hong, and Y. Cai, "Energy Efficiency Optimization for MISO SWIPT Systems With Zero-Forcing Beamforming," *IEEE Trans. Signal Process.*, vol. 64, no. 4, pp. 842–854, Feb 2016.

[14] J. Xu, L. Liu, and R. Zhang, "Multiuser MISO Beamforming for Simultaneous Wireless Information and Power Transfer," *IEEE Trans. Signal Process.*, vol. 62, no. 18, pp. 4798–4810, Sep. 2014.

[15] S. Timotheou, G. Zheng, C. Masouros, and I. Krikidis, "Symbol-level precoding in MISO broadcast channels for SWIPT systems," in *23rd International Conference on Telecommunications (ICT)*, May 2016, pp. 1–5.

[16] N. Janatian, I. Stupia, and L. Vandendorpe, "Joint multi-objective transmit precoding and receiver time switching design for MISO SWIPT systems," in *17th International Workshop on Signal Processing Advances in Wireless Communications (SPAWC)*, July 2016, pp. 1–5.

[17] G. Venkatraman, A. Tlli, M. Juntti, and L. Tran, "Multigroup Multicast Beamformer Design for MISO-OFDM With Antenna Selection," *IEEE Trans. Signal Proc.*, vol. 65, no. 22, pp. 5832–5847, Nov 2017.

[18] E. Karipidis, N. D. Sidiropoulos, and Zhi-Quan Luo, "Convex Transmit Beamforming for Downlink Multicasting to Multiple Co-Channel Groups," in *2006 IEEE International Conference on Acoustics Speech and Signal Processing Proceedings*, May 2006, vol. 5, pp. V–V.

[19] M. Alodeh, S. Chatzinotas, and B. Ottersten, "User Selection for Symbol-Level Multigroup Multicasting Precoding in the Downlink of MISO Channels," in *IEEE International Conference on Communications (ICC)*, May 2018, pp. 1–7.

[20] D. Christopoulos, S. Chatzinotas, and B. Ottersten, "Weighted Fair Multicast Multigroup Beamforming under Per-antenna Power Constraints," *IEEE Trans. Signal Process.*, vol. 62, no. 19, pp. 5132–5142, 2014.

[21] A. Z. Yalcin and M. Yuksel, "Precoder Design For Multi-Group Multicasting With a Common Message," *IEEE Trans. Comm.*, vol. 67, no. 10, pp. 7302–7315, Oct 2019.

[22] Ö. T. Demir and T. E. Tuncer, "Multi-group multicast beamforming for simultaneous wireless information and power transfer," in *23rd*

European Signal Processing Conference (EUSIPCO), Aug 2015, pp. 1356–1360.

[23] Ö. T. Demir and T. E. Tuncer, "Antenna Selection and Hybrid Beamforming for Simultaneous Wireless Information and Power Transfer in Multi-Group Multicasting Systems," *IEEE Trans. Wireless Comm.*, vol. 15, no. 10, pp. 6948–6962, Oct 2016.

[24] M. Alodeh, D. Spano, A. Kalantari, C. G. Tsinos, D. Christopoulos, S. Chatzinotas, and B. Ottersten, "Symbol-Level and Multicast Precoding for Multiuser Multiantenna Downlink: A State-of-the-Art, Classification, and Challenges," *IEEE Commun. Surveys Tuts.*, vol. 20, no. 3, pp. 1733–1757, thirdquarter 2018.

[25] M. R. A. Khandaker and K. Wong, "SWIPT in MISO Multicasting Systems," *IEEE Wireless Commun. Lett.*, vol. 3, no. 3, pp. 277–280, June 2014.

[26] D. Mishra, G. C. Alexandropoulos, and S. De, "Energy Sustainable IoT With Individual QoS Constraints Through MISO SWIPT Multicasting," *IEEE Internet Things J.*, vol. 5, no. 4, pp. 2856–2867, Aug 2018.

[27] S. Gautam, E. Lagunas, S. Chatzinotas, and B. Ottersten, "Wireless Multi-group Multicast Precoding with Selective RF Energy Harvesting," in *27th European Signal Processing Conference (EUSIPCO)*. IEEE, 2019, http://orbilu.uni.lu/handle/10993/39760.

[28] E. Karipidis, N. D. Sidiropoulos, and Z. Luo, "Far-Field Multicast Beamforming for Uniform Linear Antenna Arrays," *IEEE Trans. Signal Proc.*, vol. 55, no. 10, pp. 4916–4927, Oct 2007.

[29] D. Christopoulos, S. Chatzinotas, and B. Ottersten, "Multicast Multigroup Precoding and User Scheduling for Frame-Based Satellite Communications," *IEEE Trans. Wireless Comm.*, vol. 14, no. 9, pp. 4695–4707, Sep. 2015.

[30] H. Zhou and M. Tao, "Joint multicast beamforming and user grouping in massive MIMO systems," in *2015 IEEE International Conference on Communications (ICC)*, June 2015, pp. 1770–1775.

[31] B. Clerckx and E. Bayguzina, "Waveform Design for Wireless Power Transfer," *IEEE Trans. Signal Process.*, vol. 64, no. 23, pp. 6313–6328, 2016.

[32] X. Zhou, R. Zhang, and C. K. Ho, "Wireless Information and Power Transfer: Architecture Design and Rate-Energy Tradeoff," *IEEE Trans. Comm.*, vol. 61, no. 11, pp. 4754–4767, November 2013.

[33] J. Guo, H. Zhang, and X. Zhu, "Theoretical analysis of RF-DC conversion efficiency for class-F rectifiers," *IEEE Trans. Microw. Theory Techn.*, vol. 62, no. 4, pp. 977–985, 2014.

[34] S. Gautam, E. Lagunas, S. Chatzinotas, and B. Ottersten, "Relay Selection and Resource Allocation for SWIPT in Multi-User OFDMA Systems," *IEEE Trans. Wireless Comm.*, vol. 18, no. 5, pp. 2493–2508, May 2019.

[35] A. Wiesel, Y. C. Eldar, and S. Shamai, "Linear precoding via conic optimization for fixed MIMO receivers," *IEEE Trans. Signal Process.*, vol. 54, no. 1, pp. 161–176, Jan 2006.

[36] S. Boyd and L. Vandenberghe, *Convex optimization*, Cambridge university press, 2004.

[37] M. Grant and S. Boyd, "CVX: Matlab software for disciplined convex programming, version 2.1," http://cvxr.com/cvx, Mar. 2014.

[38] M. Grant and S. Boyd, "Graph implementations for nonsmooth convex programs," in *Recent Advances in Learning and Control*, V. Blondel, S. Boyd, and H. Kimura, Eds., Lecture Notes in Control and Information Sciences, pp. 95–110. Springer-Verlag Limited, 2008, http://stanford.edu/~boyd/graph_dcp.html.

[39] M. Bengtsson and B. Ottersten, "Optimum and Suboptimum Transmit Beamforming," in *Handbook of Antennas in Wireless Communications*. CRC press, 2001.

[40] K. Krishnan, *Linear programming (LP) approaches to semidefinite programming (SDP) problems*, Ph.D. thesis, Citeseer, 2002.

[41] FCC Notice of Proposed Rule Making, "Revision of Part 15 of the Commissions Rules Regarding Ultrawideband Transmission Systems," https://transition.fcc.gov/Bureaus/Engineering_Technology/Orders/2002/fcc02048.pdf, Apr. 2002.

[42] L. Zhang, Y. Xin, and Y.-C. Liang, "Weighted sum rate optimization for cognitive radio MIMO broadcast channels," *IEEE Trans. Wireless Comm.*, vol. 8, no. 6, pp. 2950–2959, 2009.

[43] P. Series, "Propagation data and prediction methods for the planning of indoor radiocommunication systems and radio local area networks in the frequency range 900 MHz to 100 GHz," *Recommendation ITU-R*, pp. 1238–7, 2012.

[44] R. Madani, G. Fazelnia, and J. Lavaei, "Rank-2 matrix solution for semidefinite relaxations of arbitrary polynomial optimization problems," *constraints*, vol. 21, pp. 25, 2014.

[45] A. Bozorgchenani, D. Tarchi, and G. E. Corazza, "Centralized and Distributed Architectures for Energy and Delay Efficient Fog Network-Based Edge Computing Services," *IEEE Trans. Green Commun. Netw.*, vol. 3, no. 1, pp. 250–263, March 2019.

[46] Y. Yang, Z. Liu, X. Yang, K. Wang, X. Hong, and X. Ge, "POMT: Paired Offloading of Multiple Tasks in Heterogeneous Fog Networks," *IEEE Internet Things J.*, vol. 6, no. 5, pp. 8658–8669, Oct 2019.

[47] AIR802, "IEEE 802.11 a/b/g/n WiFi Standards and Facts ," https://www.air802.com/ieee-802.11-standards-facts-amp-channels.html.

[48] B. Mitchell, "Learn Exactly How "Fast" a Wi-Fi Network Can Move," 2019, https://www.lifewire.com/how-fast-is-a-wifi-network-816543.

Sumit Gautam (S'14) received the B.Tech. degree (Hons.) in electronics and communication engineering from the LNM Institute of Information Technology (Deemed University), Jaipur, Rajasthan, India in 2013 and the MS degree in electronics and communication engineering by research from the International Institute of Information Technology (Deemed University), Hyderabad, Telangana, India in 2017. He is currently pursuing the Ph.D. degree in computer science from the Interdisciplinary Centre for Security, Reliability, and Trust (SnT), University of Luxembourg, Luxembourg. His research interests include simultaneous wireless transmission of information and energy (Wi-TIE), caching, optimization methods, cooperative communications, and precoding for multi-group multicast systems.

Eva Lagunas (S'09-M'13-SM'18) received the M.Sc. and Ph.D. degrees in telecommunications engineering from the Polytechnic University of Catalonia (UPC), Barcelona, Spain, in 2010 and 2014, respectively. She was Research Assistant within the Department of Signal Theory and Communications, UPC, from 2009 to 2013. During the summer of 2009 she was a guest research assistant within the Department of Information Engineering, Pisa, Italy. From November 2011 to May 2012 she held a visiting research appointment at the Center for Advanced Communications (CAC), Villanova University, PA, USA. In 2014, she joined the Interdisciplinary Centre for Security, Reliability and Trust (SnT), University of Luxembourg, where she currently holds a Research Scientist position. Her research interests include radio resource management and general wireless networks optimization.

Ashok Bandi (S'18) was born in Kunkalagunta, Andhra Pradesh, India, in 1988. He received the M.Tech. degree in electronics and communication engineering from the National Institute of Technology (NIT), Tiruchirappalli, India, in 2012. He has worked on Physical layer design and development for WLAN 802.11a/n/ac at Imgaination Technologies, Hyderabad, India from 2012 to 2015 and at National Instruments, Bangalore, India (2015-2016). He was worked as a project associate in the department of ECE from 2016 to May 2017. He is currently pursuing the Ph.D. degree in electrical engineering with the University of Luxembourg. He joined the Interdisciplinary Centre for Security, Reliability, and Trust, University of Luxembourg, Luxembourg, in June 2017. He is working on sparse signal Recovery and joint update of integer and non-linear variables in MINLP problems that apprear in for Wireless communications within the Project PROSAT (on-board PROcessing techniques for high throughput SATellites), funded under FNR CORE-PPP Framework.

This article has been accepted for publication in a future issue of this journal, but has not been fully edited. Content may change prior to final publication. Citation information: DOI 10.1109/OJCOMS.2019.2962077, IEEE Open Journal of the Communications Society

> OJCOMS-00052-2019 <
16

Symeon Chatzinotas (S'06-M'09-SM'13) is currently the Deputy Head of the SIGCOM Research Group, Interdisciplinary Centre for Security, Reliability, and Trust, University of Luxembourg, Luxembourg and Visiting Professor at the University of Parma, Italy. He received the M.Eng. degree in telecommunications from the Aristotle University of Thessaloniki, Thessaloniki, Greece, in 2003, and the M.Sc. and Ph.D. degrees in electronic engineering from the University of Surrey, Surrey, U.K., in 2006 and 2009, respectively. He was involved in numerous Research and Development projects for the Institute of Informatics Telecommunications, National Center for Scientific Research Demokritos, the Institute of Telematics and Informatics, Center of Research and Technology Hellas, and the Mobile Communications Research Group, Center of Communication Systems Research, University of Surrey. He has over 300 publications, 3000 citations, and an H-Index of 28 according to Google Scholar. His research interests include multiuser information theory, co-operative/cognitive communications, and wireless networks optimization. He was a co-recipient of the 2014 IEEE Distinguished Contributions to Satellite Communications Award, the CROWNCOM 2015 Best Paper Award and the 2018 EURASIC JWCN Best Paper Award.

Thang X. Vu (S'11–M'15) was born in Hai Duong, Vietnam. He received the B.S. and the M.Sc., both in Electronics and Telecommunications Engineering, from the VNU University of Engineering and Technology, Vietnam, in 2007 and 2009, respectively, and the Ph.D. in Electrical Engineering from the University Paris-Sud, France, in 2014.

From 2007 to 2009, he was with the Department of Electronics and Telecommunications, VNU University of Engineering and Technology, Vietnam as a research assistant. In 2010, he received the Allocation de Recherche fellowship to study Ph.D. in France. From September 2010 to May 2014, he was with the Laboratory of Signals and Systems (LSS), a joint laboratory of CNRS, CentraleSupelec and University Paris-Sud XI, France. From July 2014 to January 2016, he was postdoctoral researcher with the Information Systems Technology and Design (ISTD) pillar, Singapore University of Technology and Design (SUTD), Singapore. Currently, he is research associate at Interdisciplinary Centre for Security, Reliability and Trust (SnT), University of Luxembourg. His research interests are in the field of wireless communications, with particular interests of cache-assisted 5G, machine learning for communications, cloud radio access networks, and resources allocation and optimization.

Shree Krishna Sharma (S'12-M'15-SM'18) is currently Research scientist at the SnT, University of Luxembourg. Prior to this, he worked as a Postdoctoral Fellow at the University of Western Ontario, Canada, and also worked as a Research Associate at the SnT being involved in different European, national and ESA projects after receiving his PhD degree in Wireless Communications from the University of Luxembourg in 2014. His current research interests include 5G and beyond wireless, Internet of Things, machine learning, edge computing and optimization of distributed communications, computing and caching resources.

He has published about 100 technical papers in scholarly journals, international conferences and book chapters, and has over 2000 google scholar citations. He is a Senior Member of IEEE and is the recipient of several prestigious awards including "FNR Award for Outstanding Scientific Publication 2019", "2018 EURASIP Best Journal Paper Award", "CROWNCOM 2015 Best Paper Award" and "FNR Award for Outstanding PhD Thesis 2015". He has been serving as a Reviewer for several international journals and conferences; as a TPC member for a number of international conferences including IEEE ICC, IEEE GLOBECOM, IEEE PIMRC, IEEE VTC and IEEE ISWCS; and an Associate Editor for IEEE Access journal. He co-organized a special session in IEEE PIMRC 2017, a workshop in IEEE SECON 2019, worked as a Track co-chair for IEEE VTC-fall 2018 conference, and published an IET book on "Satellite Communications in the 5G Era' as a lead editor.

Steven Kisseleff (S'12–M'17) received his Dipl.-Ing. (equivalent to MSc) degree in Information Technology from the Technical University of Kaiserslautern, Germany, and Dr.-Ing. (equivalent to PhD) in Electrical Engineering from the Friedrich-Alexander University of Erlangen-Nürnberg (FAU), Germany in 2011 and 2017, respectively.

He was research and teaching assistant at the Institute for Digital Communications, FAU, from October 2011 to July 2018. From November 2012 to March 2013 he was a visiting researcher at the State University of New York at Buffalo, USA and at the Broadband Wireless Networking Lab within Georgia Institute of Technology, Atlanta, USA. In 2018, Dr. Kisseleff joined the Interdisciplinary Centre for Security, Reliability and Trust (SnT), University of Luxembourg, as a Research Associate. His research interests lie in the area of digital communications, Internet-of-Things, wireless power transfer, and satellite communication.

Björn Ottersten (S'87-M'89-SM'99-F'04) was born in Stockholm, Sweden, in 1961. He received the M.S. degree in electrical engineering and applied physics from Linköping University, Linköping, Sweden, in 1986, and the Ph.D. degree in electrical engineering from Stanford University, Stanford, CA, USA, in 1990. He has held research positions with the Department of Electrical Engineering, Linköping University, the Information Systems Laboratory, Stanford University, the Katholieke Universiteit Leuven, Leuven, Belgium, and the University of Luxembourg, Luxembourg. From 1996 to 1997, he was the Director of Research with ArrayComm, Inc., a start-up in San Jose, CA, USA, based on his patented technology. In 1991, he was appointed a Professor of signal processing with the Royal Institute of Technology (KTH), Stockholm, Sweden. From 1992 to 2004, he was the Head of the Department for Signals, Sensors, and Systems, KTH, and from 2004 to 2008, he was the Dean of the School of Electrical Engineering, KTH. He is currently the Director for the Interdisciplinary Centre for Security, Reliability and Trust, University of Luxembourg.

He was a recipient of the IEEE Signal Processing Society Technical Achievement Award in 2011 and the European Research Council advanced research grant twice, in 2009-2013 and in 2017-2022. He has co-authored journal papers that received the IEEE Signal Processing Society Best Paper Award in 1993, 2001, 2006, and 2013, and seven IEEE conference papers best paper awards. He has served as an Associate Editor for the IEEE TRANSACTIONS ON SIGNAL PROCESSING and the Editorial Board of the IEEE Signal Processing Magazine. He is currently a member of the editorial boards of EURASIP Signal Processing Journal, EURASIP Journal of Advances Signal Processing and Foundations and Trends of Signal Processing. He is a fellow of EURASIP.